

1 **IMPACT OF VARYING COMMUNITY NETWORKS ON DISEASE**
2 **INVASION***

3 STEPHEN KIRKLAND[†], ZHISHENG SHUAI[‡], P. VAN DEN DRIESSCHE[§], AND XUEYING
4 WANG[¶]

5 **Abstract.** We consider the spread of an infectious disease in a heterogeneous environment,
6 modelled as a network of patches. We focus on the invasibility of the disease, as quantified by the
7 corresponding value of an approximation to the network basic reproduction number, \mathcal{R}_0 , and study
8 how changes in the network structure affect the value of \mathcal{R}_0 . We provide a detailed analysis for two
9 model networks, a star and a path, and discuss the changes to the corresponding network structure
10 that yield the largest decrease in \mathcal{R}_0 . We develop both combinatorial and matrix analytic techniques,
11 and illustrate our theoretical results by simulations with the exact \mathcal{R}_0 .

12 **Key words.** Basic reproduction number; Matrix–Tree theorem; Group inverse.

13 **AMS subject classifications.** 92D30, 92D25, 15A09, 15A18.

14 **1. Introduction.** Advanced science and technology have made our world an in-
15 creasingly connected place. Globalization and urbanization bring not only benefits,
16 but also attendant consequences such as the spread of emerging and re-emerging in-
17 fectious diseases. Historically, plague, cholera and influenza have resulted in millions
18 of human deaths, and insight into the spread and control of these diseases has shaped
19 our modern society, particularly in medicine and public health. Recent emerging dis-
20 eases such as HIV/AIDS, SARS, Ebola and COVID-19 highlight the need for scientific
21 investigations of disease spread via transport networks [43]. As disease vectors (e.g.,
22 mosquitoes and ticks) can also be carried via human/goods transportation, the out-
23 break and spread of vector-borne diseases such as dengue, Lyme disease, malaria, West
24 Nile virus, yellow fever, and Zika virus have exhibited strong spatio–temporal patterns
25 [15, 22, 26, 37, 40, 41, 42, 47] (also see the recent special issues [31, 39]), partly due
26 to the interplay between disease epidemiology and vector ecology. Spatio–temporal
27 patterns have also been observed for many waterborne diseases caused by pathogenic
28 micro–organisms such as bacteria and protozoa that are transmitted in water/river
29 networks [3, 20, 33, 38, 45, 46]. One of the main scientific challenges is to deter-
30 mine the connection between disease risk and the change of network structures (as a
31 consequence of human behavior and/or environmental uncertainty). Recent studies
32 using statistical data from climate, environmental and disease surveillance have shown
33 inconsistent and geographically variable results. For example, a discrepancy in the
34 correlation with precipitation has appeared in the literature of waterborne diseases:
35 a significant positive association between heavy rainfall and waterborne diseases is
36 often observed [9, 13, 16, 23, 32] (also see the review paper [30]), while increased
37 prevalence of waterborne diseases has also been reported as an unexpected conse-

*This work was partly funded by the NSERC Discovery Grants RGPIN–2019–05408 (SK) and RGPIN–3677–2016 (PvdD), the NSF Grant DMS-1716445 (ZS), and the Simons Foundation Grant 317407 (XW).

[†]Department of Mathematics, University of Manitoba, Winnipeg, MB, R3T 2N2, Canada (Stephen.Kirkland@umanitoba.ca).

[‡]Department of Mathematics, University of Central Florida, Orlando, FL 32816 (shuai@ucf.edu).

[§]Department of Mathematics and Statistics, University of Victoria, Victoria, BC, V8W 2Y2, Canada (pvdd@math.uvic.ca).

[¶]Department of Mathematics and Statistics, Washington State University, Pullman, WA 99164 (xueying@math.wsu.edu).

38 quence of drought [6] and the anthropogenic protection against annual flooding [10].
 39 Detailed discussions of this discrepancy, as a consequence of human behavior and/or
 40 climate change, have been surveyed in [4, 29], while rigorous scientific explanations
 41 and theoretical insights are lacking, due to the complexity and multiple time-scales.

42 Many existing studies in the literature have focused on the aggregation of disease
 43 dynamics at each geographical region (or patch) via a static movement (or commu-
 44 nity) network, either for the situation where the time scale of the dispersal among
 45 patches is much faster than the scale of patch demography/disease dynamics, or with
 46 the focus on monotonicity of disease invasibility with respect to dispersal speed or
 47 travel frequency; for example, see [1, 8, 17, 18, 19, 44]. Recently, a general result
 48 on the spectral monotonicity of a perturbed Laplacian matrix in [12] has provided a
 49 theoretical insight on the aggregation. Specifically, for a square matrix $A = Q - \mu L$,
 50 where $Q = \text{diag}\{q_k\}$ is a diagonal matrix encoding within-vertex (within-patch) pop-
 51 ulation/disease dynamics and L is a Laplacian matrix describing population dispersal
 52 among patches in a heterogeneous environment (of n patches), the monotonicity and
 53 convexity of the spectral abscissa of A , $s(A)$, with respect to dispersal speed μ is
 54 established: $\frac{ds(A)}{d\mu} \leq 0$ and $\frac{d^2s(A)}{d\mu^2} \geq 0$. The limiting behavior with a faster time
 55 scale of population/disease dynamics is like the decoupled (no movement) system,
 56 $s(A) = \max\{q_k\}$, while the limiting behavior with a faster time scale of dispersal is
 57 the u -weighted average, $s(A) = \sum_{k=1}^n u_k q_k$, where $u = (u_1, u_2, \dots, u_n)^\top$ is the nor-
 58 malized right null vector of L . As pointed out in [12], these results also are related
 59 to the reduction principle in evolution biology [2, 25] and the evolution of dispersal
 60 in patchy landscapes [27]. For many heterogeneous infectious disease models, the
 61 network basic reproduction number \mathcal{R}_0 , a threshold determining whether the disease
 62 dies out or persists, can be approximated as the u -weighted average of the individual
 63 patch reproduction numbers $\mathcal{R}_0^{(k)}$, $\mathcal{R}_0 = \sum_{k=1}^n u_k \mathcal{R}_0^{(k)}$, when the dispersal among
 64 geographic regions is faster than the disease/population dynamics; see, e.g., [17, 44]
 65 for waterborne diseases, [12, 19, 21] for general diseases of SIS or SIR type, and [8]
 66 for the analog in a continuous spatial landscape.

67 In this paper, we investigate the impact of varying community networks on disease
 68 invasion in a heterogeneous environment. Our motivation comes from the spread of
 69 a waterborne-disease such as cholera in a heterogeneous network [17, 44], in which
 70 the pathogen (the bacterium *Vibrio cholerae*) moves along water in a hydrological
 71 landscape (e.g., a river network), or the spread of directly transmitted diseases for
 72 which the host moves between regions [1]. If the network structure changes, our goal
 73 is to determine how this affects the network basic reproduction number \mathcal{R}_0 for the
 74 spatial spread of the disease. The quantity \mathcal{R}_0 is important as it usually determines
 75 a threshold for disease extinction (when $\mathcal{R}_0 < 1$) or persistence (when $\mathcal{R}_0 > 1$), and
 76 gives guidance for disease control strategies.

77 First, we consider a toy model of a 4-node path graph network with counter-
 78 intuitive numerical results showing opposite monotonicity of \mathcal{R}_0 corresponding to a
 79 bypass from upstream to downstream (e.g., due to flooding). For the reader's conve-
 80 nience, we include in the Supplementary Material (A) the model and related results
 81 from [17, 44]. As depicted in Figure 1, we consider the spread of a pathogen (e.g.,
 82 cholera) on a path network of 4 patches (vertices) with vertices 1, 2, 3, 4 sequen-
 83 tially located along a river, where vertex 1 is upstream and vertex 4 is downstream.
 84 We assume that each nonzero movement rate, m_{ij} from vertex j to vertex i , on the
 85 path has value 1. As shown in [17, 44] the associated next generation matrix takes
 86 the form $K = FV^{-1} = D_q G_W^{-1} D_r G_I^{-1}$, where F is the matrix of new infections, V

87 is the matrix of transitions, $D_q = \text{diag}\{q_i\}$, $G_W = \text{diag}\{\delta_i\} + L$, $D_r = \text{diag}\{r_i\}$
 88 and $G_I = \text{diag}\{\mu_i\}$. Here the parameters q_i , δ_i , r_i and μ_i are the linearized in-
 89 direct transmission rate (from pathogen to host), pathogen decay rate, pathogen
 90 shedding rate and decay rate of infectious host individuals in patch i , respectively,
 91 ($i = 1, 2, 3, 4$). The matrix L is the 4×4 Laplacian matrix associated with M ,
 92 i.e., $L = \text{diag}\{\sum_{j \neq i} m_{ji}\} - M$, where $M = (m_{ij})$ with $m_{ij} \geq 0$ representing the
 93 pathogen/host dispersal from patch j to patch i . Then the exact network basic repro-
 94 duction number is $\mathcal{R}_0 = \rho(FV^{-1}) = \rho(D_q G_W^{-1} D_r G_I^{-1})$, where ρ denotes the spectral
 95 radius. For simplicity, we set $r_i/\mu_i = 1, \delta_i = 1$ in each patch, with the base q_i value
 96 taken to be $q = 0.195$. In this case, the basic reproduction number in patch i is equal
 97 to q_i . We consider two scenarios in which the network has a ‘‘hot spot’’, i.e. a vertex
 98 i at which the linearized indirect transmission rate q_i (or equivalently $\mathcal{R}_0^{(i)}$) is higher
 99 than those of the other vertices, and an arc that bypasses the hot spot. In the first
 100 case (see the left plot in Figure 1), the hot spot is assumed to be located at vertex
 101 2 with an additional bypass downstream from vertex 1 to vertex 3 being included,

102 specifically, $q_1 = q_3 = q_4 = q$, $q_2 = 10q$, and $L = \begin{pmatrix} 1 + m_{31} & -1 & 0 & 0 \\ -1 & 2 & -1 & 0 \\ -m_{31} & -1 & 2 & -1 \\ 0 & 0 & -1 & 1 \end{pmatrix}$. In the

103 second case (see the right plot in Figure 1), the hot spot is located at vertex 3 and a
 104 new bypass from vertex 2 to vertex 4 is included with $q_1 = q_2 = q_4 = q$, $q_3 = 10q$ and

105 $L = \begin{pmatrix} 1 & -1 & 0 & 0 \\ -1 & 2 + m_{42} & -1 & 0 \\ 0 & -1 & 2 & -1 \\ 0 & -m_{42} & -1 & 1 \end{pmatrix}$.

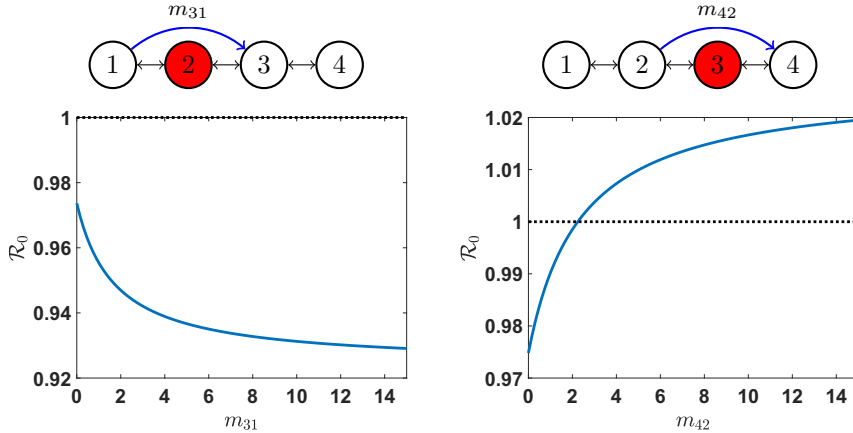


FIG. 1. With the hot spot at 2, \mathcal{R}_0 decreases as m_{31} increases (left plot); with the hot spot at 3, \mathcal{R}_0 increases as m_{42} increases (right plot).

106 In both cases the hot spot is bypassed, in the same direction, but the effects on
 107 \mathcal{R}_0 are markedly different, as shown in Figure 1. Although symmetric movement is
 108 used in the simulations for Figure 1, the inclusion of a small amount of advection
 109 (i.e., changing the subdiagonal entries to a common value slightly less than -1 to
 110 reflect the upstream-downstream movement) gives the same monotone properties of
 111 \mathcal{R}_0 . Similar behavior also occurs in the simulations of other patch disease models
 112 such as the directly transmitted disease (SIS) model in [1]; see the Supplementary
 113 Material for \mathcal{R}_0 . These unexpected behaviors motivate our investigation of the effect

114 of network structure on \mathcal{R}_0 .

115 The remainder of the article is organized as follows. Some preliminary results are
 116 provided in section 2. Two different methods, one combinatorial and one algebraic,
 117 are employed to investigate the impact of varying community networks on disease
 118 invasion, in sections 3 and 4, respectively. Applications to specific networks are il-
 119 lustrated in section 5, including an explanation of the counter-intuitive numerical
 120 results above. Disease control strategies involving varying the community network
 121 are considered in section 6, and concluding remarks are given in section 7.

122 **2. Preliminaries.** From consideration of a system of ordinary differential equa-
 123 tions governing the dynamics of cholera under the assumptions that humans become
 124 infected through contact with pathogens in the water, and that the water movement
 125 is faster than the pathogen decay rate, it has been established [17, 44] that \mathcal{R}_0 is
 126 approximated (from the exact value, given by the spectral radius of the next gen-
 127 eration matrix) by a linear combination of the basic reproduction numbers in each
 128 patch in isolation. The constants in this linear combination are the components of
 129 the normalized right eigenvector of the Laplacian matrix of the community network.
 130 The specific aim of this work is to determine how this eigenvector and \mathcal{R}_0 change with
 131 alterations in the network structure. We consider a strongly connected network, and
 132 assume that the network maintains this property when changed.

133 To be more precise, let $M = (m_{ij}) \geq 0$ denote an $n \times n$ irreducible matrix rep-
 134 resenting the pathogen/host movement in a heterogeneous environment of n patches.
 135 In particular, when $1 \leq i, j \leq n$ are distinct, $m_{ij} \geq 0$ represents the pathogen/host
 136 dispersal from patch j to patch i . We assume that $m_{ii} = 0$ for $i = 1, \dots, n$. Let
 137 $\mathcal{G} = \mathcal{G}(M)$ be the weighted digraph associated with M . That is, in \mathcal{G} there is an arc
 138 $j \rightarrow i$ from vertex j to vertex i of weight m_{ij} if and only if $m_{ij} > 0$. Let L be the
 139 Laplacian matrix of $\mathcal{G}(M)$, i.e.,

$$140 \quad (2.1) \quad L = \text{diag} \left(\sum_{i \neq 1} m_{i1}, \sum_{i \neq 2} m_{i2}, \dots, \sum_{i \neq n} m_{in} \right) - M.$$

141 Notice that each column sum of L is 0, and thus 0 is an algebraically simple eigenvalue
 142 of L (since M is irreducible). Evidently the all ones vector, $\mathbb{1}^\top$, is a left null vector for
 143 L . For each $k = 1, \dots, n$, let $C_{kk} = \det(L_{(k,k)})$ be the principal minor of L formed by
 144 deleting its k -th row and column. Consider the vector $u = (u_1, u_2, \dots, u_n)^\top$, where

$$145 \quad (2.2) \quad u_k = \frac{C_{kk}}{\sum_{\ell=1}^n C_{\ell\ell}}, \quad k = 1, \dots, n.$$

146 Denote the adjugate of L by $\text{adj}(L)$, and recall that $L \text{adj}(L) = \text{adj}(L)L = \det(L)I =$
 147 0 . Hence $\text{adj}(L) = x \mathbb{1}^\top$, where x is a nonzero vector in the right null space of L . It
 148 now follows that u is the right null vector of L , normalized so that $\mathbb{1}^\top u = 1$.

149 As shown in [17, 44] (also see [8]), when the time scale of movement is substan-
 150 tially larger than the time scale of the disease dynamics, the coefficients u_k defined
 151 above serve as weights to aggregate the disease dynamics from each patch. For this
 152 reason, u_k is called the *network risk* of patch k . In particular, the network basic re-
 153 production number \mathcal{R}_0 can be approximated by the u -weighted average of the patch
 154 basic reproduction numbers $\mathcal{R}_0^{(k)}$; that is,

$$155 \quad (2.3) \quad \mathcal{R}_0 \approx \sum_{k=1}^n u_k \mathcal{R}_0^{(k)}.$$

156 This expression (2.3) separates the structure of the movement network and the within-
 157 patch disease dynamics, and thus provides a new approach to investigate the impact
 158 of changes in the network on disease invasion. Specifically, we first investigate how
 159 a change to the network structure affects the network risks u_k , and then utilize the
 160 aggregation in (2.3) to understand how varying the network affects the disease inva-
 161 sibility (i.e., the value of \mathcal{R}_0).

162 Since u_k depends on the cofactor C_{kk} as in (2.2), it can be expressed in terms
 163 of the sum of weights of spanning rooted trees [11, 36] by using Kirchhoff’s Matrix-
 164 Tree Theorem. Calculating the weights of such trees gives a combinatorial method
 165 for finding the sign of $\frac{du_k}{dm_{ij}}$, the derivative of u_k with respect to a change in the arc
 166 $j \rightarrow i$. This combinatorial approach is developed in section 3, and may be convenient
 167 for some cases, such as small networks or networks with specific structures.

168 In addition, there is a well-established algebraic tool for understanding how
 169 changes in the movement matrix M affect the entries in the right null vector u of the
 170 Laplacian matrix L . Since L is a singular and irreducible M-matrix, the eigenvalue 0
 171 of L is algebraically simple; so, while L is not invertible, it has a *group inverse*, that
 172 is, a unique matrix $L^\#$ such that $LL^\# = L^\#L$, $LL^\#L = L$, and $L^\#LL^\# = L^\#$. The
 173 group inverse has been used effectively to analyse how changes in an irreducible non-
 174 negative matrix affect its Perron eigenvalue and eigenvector (see for example [14, 34])
 175 and our results in section 4 are informed by that approach. We refer the interested
 176 reader to [7] for background on generalized inverses in general, and to [28] for the use
 177 of the group inverses in the study of M-matrices in particular.

178 With the group inverse method developed in generality, in section 5.1, we illustrate
 179 this method with a star network in which one patch is the hub connected to several leaf
 180 vertices. Such a network structure is appropriate as a model for a large city connected
 181 to smaller cities or suburbs, with humans commuting in each direction. Then in
 182 section 5.2, we illustrate the general results for a path network, which models cholera
 183 outbreaks in communities living along a river. For these two network structures, we
 184 consider control strategies for restricted cases of the two networks (section 6), and
 185 derive results on how changes to the network can help to minimize disease invasion.

186 **3. Combinatorial method: counting spanning rooted trees.** It follows
 187 from Kirchhoff’s Matrix-Tree Theorem [11, 36] that the cofactor of the (k, k) entry
 188 of L can be interpreted in terms of spanning rooted trees:

189 (3.1)
$$C_{kk} = \sum_{\mathcal{T} \in \mathbb{T}_k} w(\mathcal{T}) =: W_k,$$

190 where \mathbb{T}_k is the set of spanning in-trees rooted at vertex k and $w(\mathcal{T}) = \prod_{(j,i) \in E(\mathcal{T})} m_{ij}$
 191 is the weight of a spanning in-tree \mathcal{T} rooted at k . The notation W_k introduced in
 192 (3.1) is convenient for tracking how $u_k = \frac{W_k}{\sum_\ell W_\ell}$, defined in (2.2), behaves as the
 193 network structure changes. Specifically, we consider a small change of the m_{ij} value
 194 (for a fixed ordered pair (i, j)) in the movement network, say $m_{ij} \rightarrow m_{ij} + \epsilon$, and
 195 explore how the value of u_k responds; to do so, we focus on the sign of $\frac{du_k}{dm_{ij}}$. (We
 196 note in passing that if m_{ij} is zero, we only consider positive values of ϵ , and in that
 197 setting $\frac{du_k}{dm_{ij}}$ is interpreted as the derivative from the right.) Notice that such a change
 198 $m_{ij} \rightarrow m_{ij} + \epsilon$ affects two entries of L ; the (i, j) entry and the (j, j) entry.

199 Before establishing our main results, we introduce some additional notation and
 200 tools from matrix theory and graph theory. Let $L_{(ij,k\ell)}$ denote the matrix obtained
 201 from L by deleting the i -th and j -th rows and k -th and ℓ -th columns. Let W_k^{ij}

202 denote the sum of the weights of all spanning in-trees rooted at k containing the arc
 203 $j \rightarrow i$, and let $W_k^{\sim ij}$ denote the sum of the weights of all spanning in-trees rooted at
 204 k that do not contain the arc $j \rightarrow i$. Notice that $W_k = W_k^{ij} + W_k^{\sim ij}$.

205 First we prove the following two lemmas.

206 LEMMA 3.1. *Assume $i \neq j$. Then*

$$207 \quad (3.2) \quad W_k^{ij} = m_{ij} |\det(L_{(ij,kj)})|.$$

208 *Proof.* From the all-minors Matrix-Tree Theorem [11], $|\det(L_{(ij,kj)})|$ is the sum
 209 of the weights of all spanning forests \mathcal{F} that contain exactly two in-tree components,
 210 one rooted at k containing vertex i and the other rooted at j . Adding the arc $j \rightarrow$
 211 i of weight m_{ij} in \mathcal{F} , yields a spanning in-tree \mathcal{T} rooted at k containing $j \rightarrow i$;
 212 in particular, $m_{ij}w(\mathcal{F}) = w(\mathcal{T})$. The identity (3.2) follows after performing this
 213 operation for all spanning forests. \square

214 We note here that strictly speaking, the right side of (3.2) is not defined in the
 215 case that $k = j$. However, we may adopt the convention that $\det(L_{(ij,kk)}) = 0$, and
 216 then (3.2) will also hold when $k = j$.

217 LEMMA 3.2. *Let $W_k = C_{kk} = \det(L_{(k,k)})$. Then, for any $i \neq j$,*

$$218 \quad (3.3) \quad \frac{dW_k}{dm_{ij}} = |\det(L_{(ij,kj)})|.$$

219 *Proof.* Straightforward calculations, along with (3.2), yield

$$\begin{aligned} 220 \quad \frac{dW_k}{dm_{ij}} &= \lim_{\epsilon \rightarrow 0} \frac{(W_k^{ij} + W_k^{\sim ij})|_{m_{ij}+\epsilon} - (W_k^{ij} + W_k^{\sim ij})|_{m_{ij}}}{\epsilon} \\ 221 &= \lim_{\epsilon \rightarrow 0} \frac{(m_{ij} + \epsilon) |\det(L_{(ij,kj)})| + W_k^{\sim ij} - m_{ij} |\det(L_{(ij,kj)})| - W_k^{\sim ij}}{\epsilon} \\ 222 &= |\det(L_{(ij,kj)})|, \end{aligned}$$

224 resulting in (3.3). \square

225 As with (3.2), when $k = j$, we interpret both sides of (3.3) as being zero.

226 In particular, if $m_{ij} > 0$ for $i \neq j$, it follows from Lemmas 3.1 and 3.2 that

$$227 \quad (3.4) \quad \frac{dW_k}{dm_{ij}} = \frac{W_k^{ij}}{m_{ij}}.$$

228

229 Now we are ready to prove the main result arising from this combinatorial method.

230 THEOREM 3.3. *For any given k, i, j , $i \neq j$,*

$$231 \quad (3.5) \quad \operatorname{sgn}\left(\frac{du_k}{dm_{ij}}\right) = \operatorname{sgn}\left(|\det(L_{(ij,kj)})| \sum_{\ell \neq k} W_\ell - W_k \sum_{\ell \neq k} |\det(L_{(ij,\ell j)})|\right).$$

232 *If, in addition, $m_{ij} > 0$, then*

$$233 \quad (3.6) \quad \operatorname{sgn}\left(\frac{du_k}{dm_{ij}}\right) = \operatorname{sgn}\left(W_k^{ij} \sum_{\ell \neq k} W_\ell^{\sim ij} - W_k^{\sim ij} \sum_{\ell \neq k} W_\ell^{ij}\right).$$

234 *Proof.* Taking the derivative on both sides of (2.2) with respect to m_{ij} yields

$$235 \quad (3.7) \quad \frac{du_k}{dm_{ij}} = \frac{1}{(\sum_{\ell} W_{\ell})^2} \left(\frac{dW_k}{dm_{ij}} \sum_{\ell} W_{\ell} - W_k \sum_{\ell} \frac{dW_{\ell}}{dm_{ij}} \right).$$

236 Substituting (3.3) into (3.7), after the cancellation of the case $\ell = k$, yields (3.5).

237 Additionally, if $m_{ij} > 0$, then it follows from (3.4) that

$$238 \quad (3.8) \quad \frac{du_k}{dm_{ij}} = \frac{1}{(\sum_{\ell} W_{\ell})^2} \left(\frac{W_k^{ij}}{m_{ij}} \sum_{\ell \neq k} W_{\ell} - W_k \sum_{\ell \neq k} \frac{W_{\ell}^{ij}}{m_{ij}} \right)$$

$$239 \quad (3.9) \quad = \frac{1}{m_{ij} (\sum_{\ell} W_{\ell})^2} \left(W_k^{ij} \sum_{\ell \neq k} (W_{\ell}^{ij} + W_{\ell}^{\sim ij}) - (W_k^{ij} + W_k^{\sim ij}) \sum_{\ell \neq k} W_{\ell}^{ij} \right)$$

$$240 \quad (3.10) \quad = \frac{1}{m_{ij} (\sum_{\ell} W_{\ell})^2} \left(W_k^{ij} \sum_{\ell \neq k} W_{\ell}^{\sim ij} - W_k^{\sim ij} \sum_{\ell \neq k} W_{\ell}^{ij} \right),$$

241

242 resulting in (3.6). \square

243 The sign identities (3.5) and (3.6) characterize how the network risk at patch k
 244 changes as a function of the movement from patch j to patch i . If more information
 245 on the movement network is provided, the exact sign of $\frac{du_k}{dm_{ij}}$ may be able to be
 246 determined. If patch k is the head of the altered arc $j \rightarrow i$ (i.e., $j = k$), then the sign
 247 of the change in the network risk $\frac{du_k}{dm_{ij}}$ is determined in the following result, regardless
 248 of the network structure.

249 **THEOREM 3.4.** *For any given $k, i, i \neq k$, $\frac{du_k}{dm_{ik}} < 0$.*

250 *Proof.* Since there is no spanning in-tree rooted at k that contains the arc $k \rightarrow i$
 251 (i.e., leaving the root vertex k), $W_k^{ij} = 0$. It follows from the irreducibility of M that
 252 there exists at least one spanning in-tree rooted at k , which certainly does not contain
 253 the arc $k \rightarrow i$; thus $W_k^{\sim ik} > 0$. If $m_{ik} > 0$, then there exists at least one vertex $\ell \neq k$
 254 at which a spanning in-tree containing $k \rightarrow i$ is rooted, and hence $W_{\ell}^{ik} > 0$. It follows
 255 from (3.6) that $\frac{du_k}{dm_{ik}} < 0$.

256 If $m_{ik} = 0$, then (3.5) can be utilized to establish the result. Specifically, there
 257 is no spanning forest of two components both of which are rooted at k , which is
 258 reflected in our convention that $\det(L_{(ij, kk)}) = 0$. Similarly, the irreducibility of M
 259 implies that $W_k > 0$ and $|\det(L_{(ij, \ell k)})| > 0$ for some $\ell \neq k$. \square

260 Notice that none of the in-trees rooted at k include the arc $k \rightarrow i$, so any increase
 261 of m_{ik} does not alter W_k but increases all other $W_{\ell}, \ell \neq k$. Consequently, all terms
 262 in the first sum of (3.5) or (3.6) vanish, as shown in the proof of Theorem 3.4. In
 263 contrast, perturbations of m_{kj} change W_k and other $W_{\ell}, \ell \neq k$, which requires more
 264 discussion.

265 If patch k is the tail of the altered arc $j \rightarrow i$ (i.e., $k = i$), and the restriction is
 266 added that the only path from j to k is the arc $j \rightarrow k$, then the proof of the following
 267 result proceeds by an analysis similar to that used to prove Theorem 3.4.

268 **THEOREM 3.5.** *For any given $k, j, j \neq k$, if the arc $j \rightarrow k$ is the only path from*
 269 *j to k , then $W_k^{\sim kj} = 0$, and $\frac{du_k}{dm_{kj}} > 0$.*

270 In section 4, we generalize Theorem 3.5 by using the group inverse to remove the
 271 restriction on the number of paths from j to k .

272 **4. Algebraic method: computing the group inverse.** Suppose that L is an
 273 irreducible Laplacian matrix with zero column sums, as in (2.1). Recall from section
 274 2 that there is a unique group inverse $L^\#$ such that $LL^\# = L^\#L$, $LL^\#L = L$, and
 275 $L^\#LL^\# = L^\#$. The left and right null spaces of L are necessarily one-dimensional,
 276 and are spanned by $\mathbb{1}^\top$ and u , respectively, where $u = (u_1, \dots, u_n)^\top$ is the right null
 277 vector of L , normalized so that $\mathbb{1}^\top u = \sum_{i=1}^n u_i = 1$. From Corollary 7.2.1 of [7], it
 278 now follows that $L^\#L = I - u\mathbb{1}^\top$.

279 Consider a perturbation $\tilde{L} = L + E$ of L such that \tilde{L} is also a singular and
 280 irreducible M-matrix with $\mathbb{1}^\top \tilde{L} = 0$. We seek the normalized right null vector of \tilde{L} ;
 281 i.e., the vector \tilde{u} such that $\tilde{L}\tilde{u} = 0$ and $\mathbb{1}^\top \tilde{u} = 1$. Since $(L + E)\tilde{u} = 0$, we have
 282 $L^\#(L + E)\tilde{u} = 0$, and hence $(I - u\mathbb{1}^\top)\tilde{u} + L^\#E\tilde{u} = 0$. Thus $(I + L^\#E)\tilde{u} = u$. Since
 283 $I + L^\#E$ is invertible (see [34], or Lemma 5.3.1 in [28]), this gives

$$284 \quad (4.1) \quad \tilde{u} = (I + L^\#E)^{-1}u.$$

285 At the end of this section, we provide an explicit expression for $L^\#$.

286 The following technical results (e.g., see [24, p.19] [35, p.475]) are useful in proving
 287 Theorem 4.2 below.

288 **LEMMA 4.1.** *Let x and y be column vectors of dimension n , then*
 289 $\det(I + xy^\top) = 1 + y^\top x$. *If in addition, $y^\top x \neq -1$, then $(I + xy^\top)^{-1} = I - \frac{1}{1 + y^\top x}xy^\top$.*
 290

291 Here is one of the main results in this section.

292 **THEOREM 4.2.** *Let L be an irreducible M-matrix as defined in (2.1).*

293 a) *Suppose that $L + \epsilon F$ is an irreducible M-matrix with $\mathbb{1}^\top F = 0$ for all ϵ in a*
 294 *neighborhood of 0. Then the directional derivative of u with respect to F is $-L^\#Fu$.*
 295 b) *Perturb $m_{ij} \rightarrow m_{ij} + \epsilon$ (where $\epsilon \geq 0$ when $m_{ij} = 0$) with $1 \leq i \neq j \leq n$, and denote*
 296 *the corresponding right null vector for the Laplacian (normalized to have sum 1) by*
 297 \tilde{u} . *Then for $k = 1, \dots, n$,*

$$298 \quad (4.2) \quad \tilde{u}_k - u_k = -\frac{\epsilon u_j e_k^\top L^\#(e_j - e_i)}{1 + \epsilon e_j^\top L^\#(e_j - e_i)} = -\frac{\epsilon u_j (L_{kj}^\# - L_{ki}^\#)}{1 + \epsilon (L_{jj}^\# - L_{ji}^\#)}.$$

299 Moreover,

$$300 \quad (4.3) \quad \frac{du_k}{dm_{ij}} = -u_j e_k^\top L^\#(e_j - e_i) = -u_j (L_{kj}^\# - L_{ki}^\#), \quad k = 1, \dots, n,$$

$$301 \quad \text{and } \frac{1}{u_j} \frac{du_k}{dm_{ij}} = -\frac{1}{u_i} \frac{du_k}{dm_{ji}}, \quad k = 1, \dots, n.$$

302 *Proof.* a) For ϵ sufficiently small,

$$303 \quad (4.4) \quad (I + \epsilon L^\#F)^{-1} = I - \epsilon L^\#F + O(\epsilon^2).$$

304 Taking $E = \epsilon F$ in (4.1) and using (4.4) yields

$$305 \quad (4.5) \quad \tilde{u} = (I + L^\#E)^{-1}u = (I - \epsilon L^\#F)u + O(\epsilon^2) = u - \epsilon L^\#Fu + O(\epsilon^2).$$

306 Hence $\lim_{\epsilon \rightarrow 0} \frac{\tilde{u} - u}{\epsilon} = -L^\#Fu$, as desired.

307 b) Set $E = \epsilon(-e_i + e_j)e_j^\top$. From (4.1), it follows that $\tilde{u} = (I + L^\#E)^{-1}u$, and
 308 Lemma 4.1 gives $(I + L^\#E)^{-1} = I - \frac{\epsilon}{1 + \epsilon e_j^\top L^\#(-e_i + e_j)}L^\#(-e_i + e_j)e_j^\top$. Observe that

309 since $I + \epsilon L^\#(-e_i + e_j)e_j^\top$ is invertible, $1 + \epsilon e_j^\top L^\#(-e_i + e_j) = \det(I + \epsilon L^\#(-e_i +$
 310 $e_j)e_j^\top) \neq 0$, following Lemma 4.1. The conclusions now follow readily. \square

311 Next we discuss how to find $L^\#$. From the hypotheses on L , it is easy to see that
 312 L may be partitioned as

$$313 \quad L = \left(\begin{array}{c|c} \bar{\mathbb{1}}^\top z & -\bar{\mathbb{1}}^\top B \\ \hline -z & B \end{array} \right)$$

314 where the submatrix B of L is an $(n-1) \times (n-1)$ invertible matrix, u_1 is the first
 315 entry of u , $\bar{u} = (u_2, \dots, u_n)^\top$, $z = \frac{1}{u_1} B\bar{u}$, and $\bar{\mathbb{1}}$ is the all ones column vector of
 316 dimension $n-1$.

317 It follows from Observation 2.3.4 of [28] that

$$318 \quad (4.6) \quad L^\# = (\bar{\mathbb{1}}^\top B^{-1}\bar{u})u\mathbb{1}^\top + \left(\begin{array}{c|c} 0 & -u_1\bar{\mathbb{1}}^\top B^{-1} \\ \hline -B^{-1}\bar{u} & B^{-1} - B^{-1}\bar{u}\bar{\mathbb{1}}^\top - \bar{u}\bar{\mathbb{1}}^\top B^{-1} \end{array} \right).$$

319 Let \bar{e}_j denote the unit column vector in \mathbb{R}^{n-1} with all zero entries except the j^{th}
 320 entry, which is one. Suppose that $1 \leq i < j \leq n$; partitioning out the first entry as
 321 above gives

$$322 \quad (4.7) \quad L^\#(e_j - e_i) = \begin{cases} \left(\begin{array}{c} -u_1\bar{\mathbb{1}}^\top B^{-1}\bar{e}_{j-1} \\ B^{-1}\bar{e}_{j-1} - \bar{u}\bar{\mathbb{1}}^\top B^{-1}\bar{e}_{j-1} \end{array} \right), & \text{if } i = 1, \\ \left(\begin{array}{c} -u_1\bar{\mathbb{1}}^\top B^{-1}(\bar{e}_{j-1} - \bar{e}_{i-1}) \\ B^{-1}(\bar{e}_{j-1} - \bar{e}_{i-1}) - \bar{u}\bar{\mathbb{1}}^\top B^{-1}(\bar{e}_{j-1} - \bar{e}_{i-1}) \end{array} \right), & \text{if } 2 \leq i \leq n. \end{cases}$$

323 From (4.7), we find that $e_1^\top L^\#(e_1 - e_j) > 0$, $j = 2, \dots, n$. The rows and columns of L
 324 can be simultaneously permuted to place any index in the first position, and hence

$$325 \quad (4.8) \quad L_{jj}^\# - L_{ji}^\# > 0, \quad i, j = 1, \dots, n, \quad i \neq j.$$

326 Suppose that $1 \leq i < j \leq n$. If we perturb $m_{ij} \rightarrow m_{ij} + \epsilon$ (where $\epsilon \geq 0$ when
 327 $m_{ij} = 0$), it follows from (4.2) and (4.7) that

$$328 \quad \tilde{u}_1 - u_1 = \begin{cases} \frac{\epsilon u_1 u_j \bar{\mathbb{1}}^\top B^{-1} \bar{e}_{j-1}}{1 + \epsilon \bar{e}_{j-1}^\top (B^{-1} \bar{e}_{j-1} - \bar{u} \bar{\mathbb{1}}^\top B^{-1} \bar{e}_{j-1})}, & i = 1, \\ \frac{\epsilon u_1 u_j \bar{\mathbb{1}}^\top B^{-1} (\bar{e}_{j-1} - \bar{e}_{i-1})}{1 + \epsilon \bar{e}_{j-1}^\top [B^{-1} (\bar{e}_{j-1} - \bar{e}_{i-1}) - \bar{u} \bar{\mathbb{1}}^\top B^{-1} (\bar{e}_{j-1} - \bar{e}_{i-1})]}, & 2 \leq i \leq n. \end{cases}$$

329 For $2 \leq \ell \leq n$, we have

$$330 \quad \tilde{u}_\ell - u_\ell = \begin{cases} -\frac{\epsilon u_j \bar{e}_{\ell-1}^\top (B^{-1} \bar{e}_{j-1} - \bar{u} \bar{\mathbb{1}}^\top B^{-1} \bar{e}_{j-1})}{1 + \epsilon \bar{e}_{j-1}^\top (B^{-1} \bar{e}_{j-1} - \bar{u} \bar{\mathbb{1}}^\top B^{-1} \bar{e}_{j-1})}, & i = 1, \\ -\frac{\epsilon u_j \bar{e}_{\ell-1}^\top [B^{-1} (\bar{e}_{j-1} - \bar{e}_{i-1}) - \bar{u} \bar{\mathbb{1}}^\top B^{-1} (\bar{e}_{j-1} - \bar{e}_{i-1})]}{1 + \epsilon \bar{e}_{j-1}^\top [B^{-1} (\bar{e}_{j-1} - \bar{e}_{i-1}) - \bar{u} \bar{\mathbb{1}}^\top B^{-1} (\bar{e}_{j-1} - \bar{e}_{i-1})]}, & 2 \leq i \leq n. \end{cases}$$

331 *Remark 4.1.* By considering (4.3) and (4.8) for the cases $j = k$ and $i = k$, we
 332 find an alternate proof for Theorem 3.4, and an extension of Theorem 3.5 that goes
 333 through without the path restriction.

334 **5. Applications to specific networks.** In this section, we apply our general
 335 results to two different networks: a star network for human transportation between
 336 one hub and several leaves, and a path network for communities along a river.

337 **5.1. Star network.** First, we consider a star network with vertex 1 as the hub,
 338 and $2, 3, \dots, n$ as leaf vertices, with corresponding weights $m_{1j}, m_{j1} > 0, j = 2, \dots, n$.
 339 Assuming that a new arc from leaf $j > 1$ to leaf $i > 1$ is added, the following result
 340 shows that the direction of change of the network risk u_k at any other vertex (i.e.,
 341 $k \neq i, k \neq j$) depends only on m_{1i} and m_{1j} .

342 **THEOREM 5.1.** *For a star network, let i, j be any two distinct leaf vertices and k*
 343 *be another vertex. Then $\operatorname{sgn}\left(\frac{du_k}{dm_{ij}}\right) = \operatorname{sgn}(m_{1i} - m_{1j})$.*

344 To illustrate both combinatorial and algebraic methods in sections 3 and 4, we
 345 prove the above result using two different approaches.

346 Combinatorial Proof of Theorem 5.1: By Theorem 3.3, it suffices to determine the
 347 sign of

$$348 \quad (5.1) \quad W_k^{ij} \sum_{\ell \neq k} W_\ell^{\sim ij} - W_k^{\sim ij} \sum_{\ell \neq k} W_\ell^{ij},$$

349 which involves the weights of certain specific spanning rooted trees. As depicted in
 350 Figure 2, $W_k^{ij} = m_{k1}m_{1i}m_{ij} \prod_s m_{1s}$ and $W_k^{\sim ij} = m_{k1}m_{1i}m_{1j} \prod_s m_{1s}$, where s takes
 351 all values except $1, k, i, j$, corresponding to the unique spanning in-tree rooted at k
 352 that contains the arc $j \rightarrow i$ and does not contain the arc $j \rightarrow i$, respectively. Now
 353 we consider spanning in-trees rooted at $\ell \neq k$, containing $j \rightarrow i$ or not, which con-
 354 tributes terms appearing in the sums of (5.1). Specifically, we consider three cases:
 355 $\ell = i, \ell = j$, and all other possible values (i.e., $\ell = r$, where $r \neq k, i, j$). As de-
 356 picted in Figure 2, $W_i^{\sim ij} = m_{i1}m_{1j}m_{1k} \prod_s m_{1s}$, $W_j^{\sim ij} = m_{j1}m_{1i}m_{1k} \prod_s m_{1s}$, $W_r^{\sim ij} =$
 357 $m_{r1}m_{1i}m_{1j}m_{1k} \prod_s m_{1s}/m_{1r}$; $W_i^{ij} = m_{i1}m_{ij}m_{1k} \prod_s m_{1s} + m_{ij}m_{j1}m_{1k} \prod_s m_{1s}$,
 358 $W_j^{ij} = 0$, $W_r^{ij} = m_{r1}m_{1i}m_{ij}m_{1k} \prod_s m_{1s}/m_{1r}$. Here s takes all values except $1, k, i, j$,
 359 and notice that there are two spanning in-trees rooted at i containing $j \rightarrow i$ while no
 360 spanning in-tree rooted at j contains $j \rightarrow i$. There is immediate cancellation in (5.1)
 361 since $W_k^{ij}W_r^{\sim ij} = W_k^{\sim ij}W_r^{ij}$, for all r . After simplification, (5.1) becomes

$$362 \quad W_k^{ij} \sum_{\ell \neq k} W_\ell^{\sim ij} - W_k^{\sim ij} \sum_{\ell \neq k} W_\ell^{ij} = W_k^{ij} [W_i^{\sim ij} + W_j^{\sim ij}] - W_k^{\sim ij} [W_i^{ij} + W_j^{ij}]$$

$$363 \quad = m_{k1}m_{1i}m_{ij} \prod_s m_{1s} \left[m_{i1}m_{1j}m_{1k} \prod_s m_{1s} + m_{j1}m_{1i}m_{1k} \prod_s m_{1s} \right]$$

$$364 \quad - m_{k1}m_{1i}m_{1j} \prod_s m_{1s} \left[m_{i1}m_{ij}m_{1k} \prod_s m_{1s} + m_{ij}m_{j1}m_{1k} \prod_s m_{1s} \right]$$

$$365 \quad = m_{k1}m_{1i}m_{j1}m_{1k}m_{ij} \left(\prod_s m_{1s} \right)^2 (m_{1i} - m_{1j}),$$
 366

367 completing the proof. \square

368 Algebraic Proof of Theorem 5.1: Consider a star network with vertex 1 as the hub,
 369 and $2, 3, \dots, n$ as leaf vertices. From the hypothesis,

$$370 \quad (5.2) \quad L = \begin{pmatrix} \sum_{i \neq 1} m_{i1} & -m_{12} & -m_{13} & \dots & -m_{1n} \\ -m_{21} & m_{12} & 0 & \dots & 0 \\ -m_{31} & 0 & m_{13} & \dots & 0 \\ \vdots & \vdots & \vdots & \ddots & \vdots \\ -m_{n1} & 0 & 0 & \dots & m_{1n} \end{pmatrix}$$

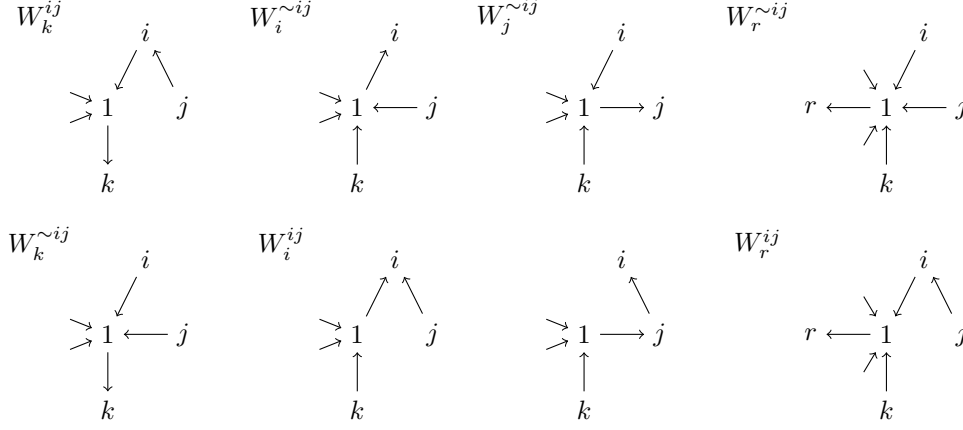


FIG. 2. Spanning rooted trees with certain specific restrictions in a star network (1 is the hub). Notice that there is no spanning in-tree rooted at j that contains the arc $j \rightarrow i$, so $W_j^{ij} = 0$.

371 For concreteness, consider $i = 2$ and $j = 3$. It follows from (4.3) that

$$372 \quad (5.3) \quad \frac{du}{dm_{23}} = -u_3 L^\#(-e_2 + e_3).$$

373 To determine the sign of $\frac{du}{dm_{23}}$, we need to compute the right hand side of (5.3). As

374 $u_3 > 0$, $\text{sgn}\left(\frac{du}{dm_{23}}\right) = \text{sgn}(-L^\#(-e_2 + e_3))$. Since $B = \text{diag}(m_{12}, \dots, m_{1n})$ is diagonal,

375 $u_1 \bar{1}^\top B^{-1}(-\bar{e}_1 + \bar{e}_2) = u_1 \left(-\frac{1}{m_{12}} + \frac{1}{m_{13}}\right)$, which implies that

$$376 \quad (B^{-1} - \bar{u} \bar{1}^\top B^{-1})(-\bar{e}_1 + \bar{e}_2) = \begin{pmatrix} -\frac{1}{m_{12}} \\ \frac{1}{m_{13}} \\ 0 \\ \vdots \\ 0 \end{pmatrix} - \begin{pmatrix} u_2 \\ u_3 \\ u_4 \\ \vdots \\ u_n \end{pmatrix} \left(-\frac{1}{m_{12}} + \frac{1}{m_{13}}\right).$$

377 So

$$378 \quad -L^\#(-e_2 + e_3) = - \left(\begin{pmatrix} -\frac{1}{m_{12}} \\ \frac{1}{m_{13}} \\ 0 \\ \vdots \\ 0 \end{pmatrix} - \begin{pmatrix} u_2 \\ u_3 \\ u_4 \\ \vdots \\ u_n \end{pmatrix} \left(-\frac{1}{m_{12}} + \frac{1}{m_{13}}\right) \right).$$

379 Thus,

$$\text{sgn}(\tilde{u}_1 - u_1) = \text{sgn}(m_{12} - m_{13}),$$

$$\text{sgn}(\tilde{u}_2 - u_2) = -\text{sgn}\left(\frac{-m_{13} - u_2(m_{12} - m_{13})}{m_{12}m_{13}}\right) = \text{sgn}(m_{13} + u_2(m_{12} - m_{13})),$$

$$380 \quad \text{sgn}(\tilde{u}_3 - u_3) = -\text{sgn}\left(\frac{m_{12} - u_3(m_{12} - m_{13})}{m_{12}m_{13}}\right) = \text{sgn}(-m_{12} + u_3(m_{12} - m_{13})),$$

$$\text{sgn}(\tilde{u}_\ell - u_\ell) = \text{sgn}\left(\frac{u_\ell(m_{12} - m_{13})}{m_{12}m_{13}}\right) = \text{sgn}(m_{12} - m_{13}), \quad \ell = 4, \dots, n.$$

381

□

382

COROLLARY 5.2. For a star network with vertex 1 as the hub, the direction of change of the network risk u_k is given by the following:

383

$$(5.4) \quad \begin{aligned} \operatorname{sgn}\left(\frac{du_k}{dm_{ij}}\right) &= \operatorname{sgn}(m_{1i} - m_{1j}), \quad k \neq i, j, i \neq 1, j \neq 1, \\ \operatorname{sgn}\left(\frac{du_i}{dm_{ij}}\right) &> 0, \operatorname{sgn}\left(\frac{du_j}{dm_{ij}}\right) < 0. \end{aligned}$$

385

5.2. River network.

386

Consider a path network with vertices labeled $1, 2, 3, \dots, n$ consecutively located along a river, where 1 denotes the vertex that is farthest upstream and n is the vertex that is farthest downstream. Suppose further that the associated movement matrix M is constant along its superdiagonal and constant along its subdiagonal. (This corresponds to constant dispersal rates for upstream and downstream movement.) The corresponding Laplacian matrix \hat{L} is given by

387

388

389

390

$$(5.5) \quad \hat{L} = \begin{pmatrix} a & -b & 0 & \cdots & 0 & 0 \\ -a & a+b & -b & \cdots & 0 & 0 \\ 0 & -a & a+b & \cdots & 0 & 0 \\ \vdots & \vdots & & & & \\ 0 & 0 & 0 & \cdots & a+b & -b \\ 0 & 0 & 0 & \cdots & -a & b \end{pmatrix}$$

392

for $a > 0$ and $b > 0$. It suffices to consider the case that $a \geq b$; see Supplementary Material (B) for a justification. Henceforth we restrict to the case that $a \geq b$.

393

394

Setting $\alpha = \frac{a}{b}$ yields

$$(5.6) \quad \hat{L} = b \begin{pmatrix} \alpha & -1 & 0 & \cdots & 0 & 0 \\ -\alpha & \alpha+1 & -1 & \cdots & 0 & 0 \\ 0 & -\alpha & \alpha+1 & \cdots & 0 & 0 \\ \vdots & \vdots & & & & \\ 0 & 0 & 0 & \cdots & \alpha+1 & -1 \\ 0 & 0 & 0 & \cdots & -\alpha & 1 \end{pmatrix} := bL.$$

396

397

398

399

400

401

Our assumption that $a \geq b$ gives $\alpha \geq 1$, and we note that this fits with our interpretation of 1 being an upstream vertex and n being a downstream vertex. It is readily verified that the vector $u = (u_1, u_2, \dots, u_n)^\top = \frac{1}{\sum_{\ell=0}^{n-1} \alpha^\ell} (1, \alpha, \alpha^2, \dots, \alpha^{n-1})^\top$ is the right null vector of L normalized so that $\mathbf{1}^\top u = 1$. Let B denote the principal submatrix of L formed by deleting the first row and column. A proof by induction on n shows that the (k, j) entry of B^{-1} is given by

402

$$\bar{e}_k^\top B^{-1} \bar{e}_j = \begin{cases} 1 + \alpha + \alpha^2 + \cdots + \alpha^{k-1}, & 1 \leq k \leq j \leq n-1, \\ \alpha^{k-j} (1 + \alpha + \alpha^2 + \cdots + \alpha^{j-1}), & 1 \leq j < k \leq n-1. \end{cases}$$

403

It can be shown by induction on n that the sum of the entries in column j of B^{-1} is

404

$$\bar{\mathbf{1}}^\top B^{-1} \bar{e}_j = j \sum_{\ell=0}^{n-j-1} \alpha^\ell + \sum_{\ell=n-j}^{n-2} (n-1-\ell) \alpha^\ell, \quad j = 1, 2, \dots, n-1$$

405

where the empty sum is interpreted as zero.

406

The following is straightforward.

407 LEMMA 5.3. *Suppose that $m \geq 0$ and $n \in \mathbb{N}$. Then*

$$408 \left(\sum_{\ell=0}^m \alpha^\ell \right) \left(\sum_{\ell=0}^{n-1} \alpha^\ell \right) = \sum_{\ell=0}^m (\ell+1) \alpha^\ell + (m+1) \sum_{\ell=m+1}^{n-1} \alpha^\ell + \sum_{\ell=n}^{n+m-1} (n+m-\ell) \alpha^\ell.$$

409 The following can be deduced from (4.7) and our expression for B^{-1} .

410 LEMMA 5.4. *For a path network, if $1 \leq i < j \leq n$, then*

$$411 L_{jj}^\# - L_{ji}^\# = \frac{\sum_{\ell=0}^{j-i-1} (\ell+1) \alpha^\ell + (j-i) \sum_{\ell=j-i}^{j-2} \alpha^\ell}{\sum_{\ell=0}^{n-1} \alpha^\ell}.$$

412 Lemmas 5.3 and 5.4, along with (4.7) establish the following result.

413 THEOREM 5.5. *On a path network, if $1 \leq k \leq j \leq n$, then*

$$414 e_k^\top L^\#(e_j - e_1) =$$

$$415 \frac{1}{\sum_{\ell=0}^{n-1} \alpha^\ell} \left(\sum_{\ell=0}^{k-2} (\ell+1) \alpha^\ell - (j-k) \sum_{\ell=k-1}^{n+k-j-1} \alpha^\ell - \sum_{\ell=n-j+k}^{n-2} (n-\ell-1) \alpha^\ell \right).$$

416 For $j < k \leq n$,

$$417 e_k^\top L^\#(e_j - e_1) = \alpha^{k-j} e_j^\top L^\#(e_j - e_1) = \frac{\alpha^{k-j}}{\sum_{\ell=0}^{n-1} \alpha^\ell} \left(\sum_{\ell=0}^{j-2} (\ell+1) \alpha^\ell \right).$$

418

419 Theorem 5.5 yields the following result.

420 COROLLARY 5.6. *For $1 \leq k \leq j-1$,*

$$421 (e_{k+1}^\top - e_k^\top) L^\#(e_j - e_1) = \frac{\alpha^{k-1}}{\sum_{\ell=0}^{n-1} \alpha^\ell} \left(j + \sum_{\ell=1}^{n-j} \alpha^\ell \right) > 0.$$

$$422 \text{ For } j \leq k \leq n-1, (e_{k+1}^\top - e_k^\top) L^\#(e_j - e_1) = \frac{\alpha^{k-j}}{\sum_{\ell=0}^{n-1} \alpha^\ell} \left(\sum_{\ell=0}^{j-2} (\ell+1) \alpha^\ell \right) (\alpha - 1) > 0.$$

423 *Remark 5.1.* Set $\tilde{L} = L + \epsilon(e_j - e_1)e_j^\top$ with $1 < j \leq n$ and $\epsilon > 0$ so that
 424 $\tilde{u} - u = -cL^\#(e_j - e_1)$ where $c = \frac{\epsilon u_j}{1 + \epsilon(L_{jj}^\# - L_{j1}^\#)} > 0$ by Theorem 4.2 b). By Theorem
 425 5.5, $\tilde{u}_1 - u_1 > 0$ and $\tilde{u}_k - u_k < 0, j \leq k \leq n$. It follows from Corollary 5.6 that $\tilde{u}_k - u_k$
 426 is decreasing in k if $\alpha > 1$. If $\alpha = 1$, $\tilde{u}_k - u_k$ is decreasing in k for $1 \leq k \leq j$ and
 427 constant for $j \leq k \leq n$.

428 Next we consider $L^\#(e_j - e_i)$ for $j, i > 1$. The proofs again rely on (4.7) and our
 429 expression for B^{-1} .

430 LEMMA 5.7. *For a path network with $2 \leq i < j \leq n$,*

$$431 \bar{e}_k^\top B^{-1}(\bar{e}_{j-1} - \bar{e}_{i-1}) = \begin{cases} 0, & \text{if } 1 \leq k \leq i-1, \\ \sum_{\ell=0}^{k-i} \alpha^\ell, & \text{if } i-1 < k \leq j-1, \\ \alpha^{k-j+1} \sum_{\ell=0}^{j-i} \alpha^\ell, & \text{if } j-1 < k \leq n, \end{cases}$$

432 THEOREM 5.8. *On a path network, if $2 \leq i < j \leq n$, then*

$$433 \quad e_k^\top L^\#(e_j - e_i) = -\frac{\alpha^{k-1}}{\sum_{\ell=0}^{n-1} \alpha^\ell} \left((j-i) \sum_{\ell=0}^{n-j} \alpha^\ell + \sum_{\ell=n-j+1}^{n-i-1} (n-i-\ell) \alpha^\ell \right)$$

434 *for $1 \leq k \leq i$. For $i < k \leq j$,*

$$435 \quad e_k^\top L^\#(e_j - e_i) = \frac{1}{\sum_{\ell=0}^{n-1} \alpha^\ell} \left(\sum_{\ell=0}^{k-i-1} (\ell+1) \alpha^\ell + (k-i) \sum_{\ell=k-i}^{k-2} \alpha^\ell \right. \\ 436 \quad \left. - (j-k) \sum_{\ell=k-1}^{n+k-j-1} \alpha^\ell - \sum_{\ell=n-j+k}^{n-2} (n-1-\ell) \alpha^\ell \right).$$

437 *For $j < k \leq n$, $e_k^\top L^\#(e_j - e_i) = \alpha^{k-j} e_j^\top L^\#(e_j - e_i) = \frac{\alpha^{k-j}}{\sum_{\ell=0}^{n-1} \alpha^\ell} \left(\sum_{\ell=0}^{j-i-1} (\ell+1) \alpha^\ell \right.$
438 $\left. + (j-i) \sum_{\ell=j-i}^{j-2} \alpha^\ell \right)$.*

439 COROLLARY 5.9. *If $2 \leq i < j \leq n$, then $(e_{k+1} - e_k^\top) L^\#(e_j - e_i) =$*

$$440 \quad \begin{cases} -\frac{\alpha^{k-1}}{\sum_{\ell=0}^{n-1} \alpha^\ell} \left((j-i) \sum_{\ell=0}^{n-j} \alpha^\ell + \sum_{\ell=n-j+1}^{n-i-1} (n-i-\ell) \alpha^\ell \right) (\alpha-1) \geq 0, & 1 \leq k \leq i-1, \\ \frac{1}{\sum_{\ell=0}^{n-1} \alpha^\ell} \left(\sum_{\ell=0}^{i-2} \alpha^\ell + (j-i+1) \alpha^{i-1} + \sum_{\ell=i}^{n+i-j-1} \alpha^\ell \right) > 0, & k = i, \\ \frac{1}{\sum_{\ell=0}^{n-1} \alpha^\ell} \left(\sum_{\ell=k-i}^{k-2} \alpha^\ell + (j-i+1) \alpha^{k-1} + \sum_{\ell=k}^{n+k-j-1} \alpha^\ell \right) > 0, & i < k \leq k+1 \leq j, \\ \frac{\alpha^{k-j}}{\sum_{\ell=0}^{n-1} \alpha^\ell} \left(\sum_{\ell=0}^{j-2} (\ell+1) \alpha^\ell \right) (\alpha-1) \geq 0, & j \leq k \leq n-1. \end{cases}$$

441 *Remark 5.2.* Let $2 \leq i < j \leq n$ and $\epsilon > 0$. Set $\tilde{L} = L + \epsilon(e_j - e_i)e_j^\top$. It follows
442 from Theorem 4.2 b) that

$$443 \quad (5.7) \quad \tilde{u} - u = -cL^\#(e_j - e_i)$$

444 where $c = \frac{\epsilon u_j}{1 + \epsilon(L_{jj}^\# - L_{ji}^\#)} > 0$ (observe that $L_{jj}^\# - L_{ji}^\# > 0$ by (4.8)). In view of Theorem
445 5.8, we see that

$$446 \quad \tilde{u}_k - u_k = \begin{cases} \frac{c\alpha^{k-1}}{\sum_{\ell=0}^{n-1} \alpha^\ell} \left((j-i) \sum_{\ell=0}^{n-j} \alpha^\ell + \sum_{\ell=0}^{n-i-1} (n-i-\ell) \alpha^\ell \right) > 0, & 1 \leq k \leq i, \\ \frac{-c\alpha^{k-j}}{\sum_{\ell=0}^{n-1} \alpha^\ell} \left(\sum_{\ell=0}^{j-i-1} (\ell+1) \alpha^\ell + (j-i) \sum_{\ell=j-i}^{j-2} \alpha^\ell \right) < 0, & j \leq k \leq n. \end{cases}$$

447 Observe that if $i \geq 2$ and $1 \leq k \leq n-1$, $(\tilde{u}_{k+1} - u_{k+1}) - (\tilde{u}_k - u_k) = -c(e_{k+1} -$
448 $e_k^\top) L^\#(e_j - e_i)$. It now follows from Corollary 5.9 that if $\alpha > 1$, then $(\tilde{u}_{k+1} - u_{k+1}) -$
449 $(\tilde{u}_k - u_k) < 0$. Hence, if $\alpha > 1$ then $\tilde{u}_k - u_k$ is decreasing as a function of k for
450 $1 \leq k \leq n$.

451 Assume that a new arc from vertex j to vertex i is added, where $i < j$; the
452 following result shows that the network risk u_k decreases at all vertices downstream
453 from j and increases at all vertices upstream from i . The result follows readily from
454 Theorems 4.2 and 5.8.

455 THEOREM 5.10. Consider a path network, and suppose that $1 \leq i < j \leq n$. For
 456 any $k \leq i$, $\text{sgn}(\frac{du_k}{dm_{ji}}) < 0$, while for any $j < k$, $\text{sgn}(\frac{du_k}{dm_{ji}}) > 0$.

457 For the vertices k between j and i (i.e., $i < k < j$), the change of the network
 458 risk u_k depends on the position of the vertices as well as the magnitude of m_{ij} .

459 We now revisit the toy model of a path graph network described in section 1.

460 EXAMPLE 1. In this example we show how the results developed in section 4 yield
 461 insight into the toy example presented in Figure 1. We suppose that the time scale of
 462 movement greatly exceeds that of the disease dynamics, so that the asymptotic approx-
 463 imation $\mathcal{R}_0 = \sum_{k=1}^4 u_k q_k$ applies, where u denotes the null vector of the Laplacian
 464 matrix L , normalised so that $\sum_{k=1}^4 u_k = 1$. Taking $\alpha = 1$ yields

$$465 L = \begin{bmatrix} 1 & -1 & 0 & 0 \\ -1 & 2 & -1 & 0 \\ 0 & -1 & 2 & -1 \\ 0 & 0 & -1 & 1 \end{bmatrix}, \text{ and } L^\# = \frac{1}{8} \begin{bmatrix} 7 & 1 & -3 & -5 \\ 1 & 3 & -1 & -3 \\ -3 & -1 & 3 & 1 \\ -5 & -3 & 1 & 7 \end{bmatrix}. \text{ A bypass from}$$

466 vertex 1 to vertex 3 corresponds to the perturbing matrix $E = m_{31}(e_1 - e_3)e_1^\top$, and
 467 a computation now reveals that the normalised null vector of the perturbed Laplacian

$$468 \text{ matrix is given by } \tilde{u} = \frac{1}{4}\mathbb{1} - \frac{m_{31}}{16+20m_{31}} \begin{bmatrix} 5 \\ 1 \\ -3 \\ -3 \end{bmatrix}. \text{ If the hot spot is at vertex 2, with}$$

469 $q_i = q, i = 1, 3, 4, q_2 = 10q$, then $\mathcal{R}_0 = \sum_{k=1}^4 \tilde{u}_k q_k = q(\frac{13}{4} - \frac{9m_{31}}{16+20m_{31}})$; evidently this
 470 is decreasing and concave down as a function of m_{31} , as is clearly reflected in Figure
 471 1 (left plot) by computing \mathcal{R}_0 numerically.

472 Next, considering a bypass from vertex 2 to vertex 4, (so that E is given by

$$473 m_{42}(e_2 - e_4)e_2^\top) \text{ an analogous argument shows that } \tilde{u} = \frac{1}{4}\mathbb{1} - \frac{m_{42}}{16+12m_{42}} \begin{bmatrix} 3 \\ 3 \\ -1 \\ -5 \end{bmatrix}.$$

474 With vertex 3 as the hot spot and $q_i = q, i = 1, 2, 4, q_3 = 10q$, it now follows that
 475 $\sum_{k=1}^4 \tilde{u}_k q_k = q(\frac{13}{4} + \frac{9m_{42}}{16+12m_{42}})$. Evidently this last is increasing and concave down as
 476 a function of m_{42} , as depicted in Figure 1 (right plot).

477 Alternatively, as u_k encodes the weights of spanning in-trees rooted at k , as shown
 478 in section 3, both bypasses (from vertex 1 to vertex 3 or from vertex 2 to vertex 4)
 479 increase u_1 and u_2 but decrease u_3 and u_4 . For example, with the bypass from vertex
 480 1 to vertex 3 of weight m_{31} , we have

$$481 u_1 = \frac{m_{12}m_{23}m_{34}}{\Delta} = \frac{1}{4+5m_{31}} = \frac{1}{4} - \frac{\frac{5}{4}m_{31}}{4+5m_{31}},$$

$$482 u_2 = \frac{m_{21}m_{23}m_{34} + m_{23}m_{31}m_{34}}{\Delta} = \frac{1+m_{31}}{4+5m_{31}} = \frac{1}{4} - \frac{\frac{1}{4}m_{31}}{4+5m_{31}},$$

$$483 u_3 = \frac{m_{34}m_{32}m_{21} + m_{34}m_{31}m_{12} + m_{34}m_{31}m_{32}}{\Delta} = \frac{1+2m_{31}}{4+5m_{31}} = \frac{1}{4} + \frac{\frac{3}{4}m_{31}}{4+5m_{31}},$$

$$484 u_4 = \frac{m_{43}m_{32}m_{21} + m_{43}m_{32}m_{31} + m_{43}m_{31}m_{12}}{\Delta} = \frac{1+2m_{31}}{4+5m_{31}} = \frac{1}{4} + \frac{\frac{3}{4}m_{31}}{4+5m_{31}},$$

486 where Δ is the sum of weights of spanning in-trees rooted at any vertex, that is, $\Delta =$
 487 $m_{12}m_{23}m_{34} + m_{21}m_{23}m_{34} + m_{23}m_{31}m_{34} + m_{34}m_{32}m_{21} + m_{34}m_{31}m_{12} + m_{34}m_{31}m_{32} +$

488 $m_{43}m_{32}m_{21} + m_{43}m_{32}m_{31} + m_{43}m_{31}m_{12} = 4 + 5m_{31}$. A location of a hot spot at
 489 vertex 1 or 2 leads to the decrease of \mathcal{R}_0 due to the bypass, while a hot spot at vertex
 490 3 or 4 leads to the increase of \mathcal{R}_0 .

491 **EXAMPLE 2.** Consider a path network on 5 vertices with an additional arc from
 492 vertex 2 to vertex 4 being added. All other settings are the same as in Example 1.
 493 Figure 3 shows how \mathcal{R}_0 responds to this addition in the scenarios of the disease hot
 494 spot, located at various different vertices. It turns out that when vertex 3 is the hot
 495 spot, there is no change in \mathcal{R}_0 , no matter how large the value of m_{24} is. When the
 496 time scale of movement greatly exceeds that of the disease dynamics, the results of
 497 sections 3 and 4 explain Figure 3. For example, the bypass decreases u_1 and u_2 but
 498 increases u_4 and u_5 . Therefore, a hot spot at vertex 1 or 2 leads to a decrease of \mathcal{R}_0
 499 while a hot spot at vertex 4 or 5 leads to an increase of \mathcal{R}_0 , due to the bypass.

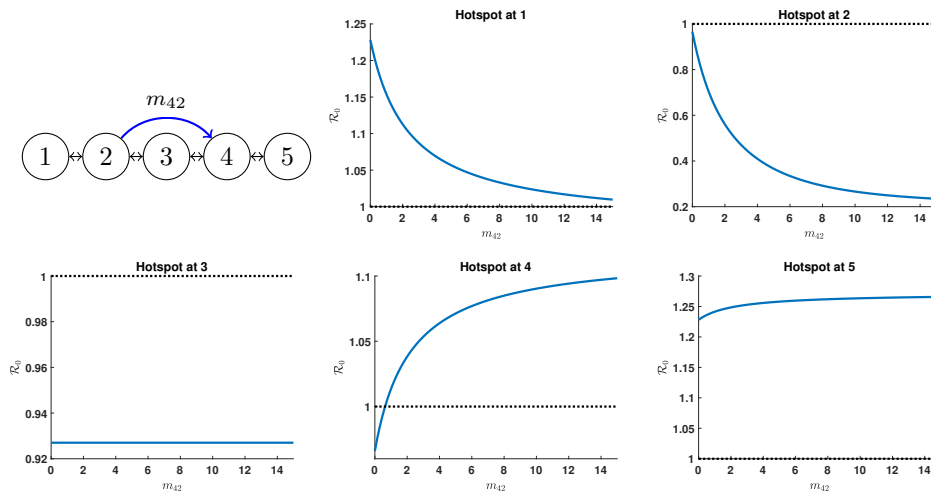


FIG. 3. The impact of a bypass in a path network of 5 vertices.

500 Motivated by the observation made in Example 2 for the case that vertex 3 is
 501 the hot spot, we use the exact network basic reproduction number to prove a general
 502 result below, from which the observation is readily recovered.

503 **THEOREM 5.11.** Suppose that M is an irreducible movement matrix and that L
 504 is the corresponding Laplacian matrix. Let $c > 0$ and $V = L + cI$. Suppose further
 505 that there is a permutation matrix Q and indices i, j such that: a) F and L both
 506 commute with Q , and b) $Qe_j = e_i$. Then for any $\epsilon > 0$, the basic reproduction numbers
 507 corresponding to M and $M + \epsilon(e_j - e_i)e_j^\top$ are equal.

508 *Proof.* Let $E = \epsilon(e_j - e_i)e_j^\top$. The network basic reproduction number correspond-
 509 ing to M is $\rho(FV^{-1})$, while that corresponding to the perturbed network $M + E$ is
 510 $\rho(F(V + E)^{-1})$. We have

$$511 \quad (5.8) \quad F(V + E)^{-1} = FV^{-1} \left(I + \epsilon(e_j - e_i)e_j^\top V^{-1} \right)^{-1}.$$

512 Observe that V is a column diagonally dominant M-matrix. From Lemma 3.14 in
 513 Chapter 9 of [5], it follows that the maximum entry in any row of V^{-1} occurs on the

514 diagonal. In particular, $e_j^\top V^{-1}(e_j - e_i) \geq 0$. It now follows that

$$515 \quad (5.9) \quad \left(I + \epsilon(e_j - e_i)e_j^\top V^{-1} \right)^{-1} = I - \frac{\epsilon}{1 + \epsilon e_j^\top V^{-1}(e_j - e_i)} (e_j - e_i)e_j^\top V^{-1}.$$

516 Substituting (5.9) into (5.8) yields

$$517 \quad F(V + E)^{-1} = FV^{-1} \left[I - \frac{\epsilon}{1 + \epsilon e_j^\top V^{-1}(e_j - e_i)} (e_j - e_i)e_j^\top V^{-1} \right]$$

$$518 \quad = FV^{-1} - \frac{\epsilon FV^{-1}(e_j - e_i)e_j^\top V^{-1}}{1 + \epsilon e_j^\top V^{-1}(e_j - e_i)}.$$

519

520 Next, consider a positive left Perron vector y for FV^{-1} , i.e. $y^\top FV^{-1} = \mathcal{R}_0 y^\top$.
 521 Since F and V both commute with Q , so does FV^{-1} . Consequently, $y^\top QFV^{-1}Q^\top =$
 522 $\mathcal{R}_0 y^\top$, implying that $(y^\top Q)FV^{-1} = \mathcal{R}_0(y^\top Q)$. Hence $y^\top Q$ is also a left Perron vector
 523 for FV^{-1} . Since that Perron vector is unique up to a scalar multiple, we find that
 524 necessarily $y^\top Q = y^\top$. In particular, $y_i = y^\top Qe_j = y^\top e_j = y_j$.

525 Now consider

$$526 \quad y^\top F(V + E)^{-1} = y^\top FV^{-1} - \frac{\epsilon y^\top FV^{-1}(e_j - e_i)e_j^\top V^{-1}}{1 + \epsilon e_j^\top V^{-1}(e_j - e_i)}$$

$$527 \quad = \mathcal{R}_0 y^\top - \frac{\epsilon \mathcal{R}_0(y_j - y_i)e_j^\top V^{-1}}{1 + \epsilon e_j^\top V^{-1}(e_j - e_i)} = \mathcal{R}_0 y^\top.$$

528

529 Hence y is a positive left eigenvector of $F(V + E)^{-1}$, (with corresponding eigen-
 530 value \mathcal{R}_0), from which it follows that $F(V + E)^{-1}$ has y as a left Perron vector and
 531 \mathcal{R}_0 as its Perron value. \square

532 *Remark 5.3.* Inspecting the proof of Theorem 5.11, we find that the conclusion
 533 holds also for negative values of ϵ , provided that $\epsilon > -m_{ij}$ and $\epsilon > -\frac{1}{e_j^\top V^{-1}(e_j - e_i)}$.

534 As an application of Theorem 5.11, consider a river network on $2k + 1$ vertices
 535 with $\alpha = 1$, and suppose that F is the diagonal matrix whose ℓ -th diagonal entry is
 536 1 for $\ell \neq k + 1$, and whose $k + 1$ -st diagonal entry is $x > 1$. Setting $V = L + cI$ for
 537 some $c > 0$, we see that V and F commute with the “back diagonal” permutation
 538 matrix P , where the $(\ell, 2k + 2 - \ell)$ entry of P is 1 for $\ell = 1, \dots, 2k + 1$. Fix an index
 539 $j = 1, \dots, 2k + 1$, and note that $Pe_j = e_{2k+2-j}$. From the above theorem, for any
 540 $\epsilon > 0$, the basic reproduction numbers associated with the movement matrices M
 541 and $M + \epsilon(e_j - e_{2k+2-j})e_j^\top$ are equal. In particular, for a river network on 5 vertices
 542 with $\alpha = 1$, adding a weighted arc from vertex 4 to vertex 2 does not affect the value
 543 of \mathcal{R}_0 . This justifies the observation made in Example 2 for the hot spot locating at
 544 vertex 3.

545 **6. Control strategies.** The techniques developed in sections 3 and 4 inform
 546 a strategy for controlling invasibility. Given an irreducible movement matrix M ,
 547 the control strategy corresponds to a perturbation of M , say $M + E$ which is also
 548 irreducible and nonnegative. Denoting the corresponding Laplacian matrices and
 549 normalized right null vectors by L, u and \tilde{L}, \tilde{u} respectively, we find that the associated
 550 network basic reproduction numbers are approximately $\mathcal{R}_0 = \sum_{k=1}^n u_k \mathcal{R}_0^{(k)}$ and $\tilde{\mathcal{R}}_0 =$
 551 $\sum_{k=1}^n \tilde{u}_k \mathcal{R}_0^{(k)}$. Our goal is then to find a suitable perturbing matrix E so as to ensure
 552 that $\tilde{\mathcal{R}}_0 - \mathcal{R}_0$ is negative and, ideally, large in absolute value.

553 From the results in section 4, we find that

$$554 \quad (6.1) \quad \tilde{\mathcal{R}}_0 - \mathcal{R}_0 = \sum_{k=1}^n (\tilde{u}_k - u_k) \mathcal{R}_0^{(k)} = \sum_{k=1}^n e_k^\top ((I + L^\# E)^{-1} - I) u \mathcal{R}_0^{(k)}.$$

555 In particular, for a perturbing matrix E , the effectiveness of the corresponding control
556 strategy in mitigating the invasion can be quantified using (6.1).

557 In this section, we focus on a restricted set of perturbations: for distinct indices
558 i, j and fixed ϵ , we consider the effect of increasing the movement rate from patch j
559 to patch i from m_{ij} to $m_{ij} + \epsilon$. In this case, (6.1) simplifies considerably: from the
560 results of section 4, it follows that in this restricted setting,

$$561 \quad (6.2) \quad \tilde{\mathcal{R}}_0 - \mathcal{R}_0 = - \frac{\epsilon u_j}{1 + \epsilon(L_{jj}^\# - L_{ji}^\#)} \sum_{k=1}^n (L_{kj}^\# - L_{ki}^\#) \mathcal{R}_0^{(k)}.$$

562 Our challenge is then to select the indices i, j so as to minimize the expression

$$563 \quad (6.3) \quad - \frac{\epsilon u_j}{1 + \epsilon(L_{jj}^\# - L_{ji}^\#)} \sum_{k=1}^n (L_{kj}^\# - L_{ki}^\#) \mathcal{R}_0^{(k)}.$$

564 We remark here that for $\epsilon > 0$, the expression (6.2) is always valid. However, for
565 negative values of ϵ , another hypothesis is required in order for the derivation of
566 (6.2) to hold. In that case, we need to assume that $-m_{ij} < \epsilon$ (otherwise there is a
567 danger that the network is no longer strongly connected). Evidently that additional
568 hypothesis is satisfied if, for example, we assume that when ϵ is negative, its absolute
569 value is sufficiently small. For ease of exposition in the sequel, we only deal with the
570 case $\epsilon > 0$ in the remainder of this section.

571 While we focus only on perturbing a single entry in the movement matrix M , note
572 that these special perturbations are building blocks: any admissible perturbation can
573 be written as a linear combination of these restricted perturbations.

574 From (6.3) it is clear that the specific values of $\mathcal{R}_0^{(k)}, k = 1, \dots, n$ are needed
575 in order to assess the effect on the basic reproduction number of changing m_{ij} to
576 $m_{ij} + \epsilon$. However, we restrict ourselves to the following situation, in which the anal-
577 ysis simplifies even further. Imagine that one patch, say ℓ , is a ‘‘hot spot’’ for the
578 disease, and that the patch reproduction numbers $\mathcal{R}_0^{(k)}, k \neq \ell$ take on a common
579 value. Formally we assume that for some index ℓ , we have $\mathcal{R}_0^{(k)} = r_0$ whenever $k \neq \ell$,
580 with $\mathcal{R}_0^{(\ell)} > r_0$. Then $\tilde{\mathcal{R}}_0 - \mathcal{R}_0 = \sum_{k=1, \dots, n, k \neq \ell} (\tilde{u}_k - u_k) \mathcal{R}_0^{(k)} + (\tilde{u}_\ell - u_\ell) \mathcal{R}_0^{(\ell)} =$
581 $r_0 \sum_{k=1, \dots, n, k \neq \ell} (\tilde{u}_k - u_k) + (\tilde{u}_\ell - u_\ell) \mathcal{R}_0^{(\ell)}$. The fact that $\sum_{k=1}^n (\tilde{u}_k - u_k) = 0$, gives

$$582 \quad (6.4) \quad \tilde{\mathcal{R}}_0 - \mathcal{R}_0 = (\tilde{u}_\ell - u_\ell) (\mathcal{R}_0^{(\ell)} - r_0).$$

583 For our restricted family of perturbations, we have $\tilde{\mathcal{R}}_0 - \mathcal{R}_0 = - \frac{\epsilon u_j}{1 + \epsilon(L_{jj}^\# - L_{ji}^\#)} (L_{\ell j}^\# -$
584 $L_{\ell i}^\#) (\mathcal{R}_0^{(\ell)} - r_0)$. Hence it suffices to select the indices i, j that maximize the expres-
585 sion $\frac{u_j}{1 + \epsilon(L_{jj}^\# - L_{ji}^\#)} (L_{\ell j}^\# - L_{\ell i}^\#)$. In subsections 6.1 and 6.2, we revisit the star and river
586 networks and discuss how these perturbations affect the basic reproduction number.

587 **6.1. Star with a hot spot.** In what follows, we assume that $\epsilon > 0$, and we con-
588 sider a special case. We assume that $m_{12} \geq m_{13} \geq \dots \geq m_{1n}$, and impose the further

589 assumption that $m_{1k} = m_{k1}$, $k = 2, \dots, n$. We note that when this is the case, $u = \frac{1}{n} \mathbb{1}$.
 590

591 *Case 1: the hot spot is located at the hub (vertex 1):*

592 We claim that the best strategy to reduce the infection risk is to increase m_{n1} when
 593 $m_{1k} = m_{k1}$ for $2 \leq k \leq n$. Perturb $m_{1j} \rightarrow m_{1j} + \epsilon$ for $\epsilon > 0$ and $1 < j \leq n$. Then

$$594 \quad \tilde{u}_1 - u_1 = -\frac{\epsilon u_j e_1^\top L^\#(e_j - e_1)}{1 + \epsilon e_j^\top L^\#(e_j - e_1)} = \frac{\epsilon u_1 u_j \bar{\mathbb{1}}^\top B^{-1} \bar{e}_{j-1}}{1 + \epsilon \bar{e}_{j-1}^\top (B^{-1} \bar{e}_{j-1} - \bar{u} \bar{\mathbb{1}}^\top B^{-1} \bar{e}_{j-1})}$$

$$595 \quad = \frac{\epsilon u_1 u_j / m_{1j}}{1 + \epsilon(1 - u_j) / m_{1j}} > 0.$$

596 Perturb $m_{i1} \rightarrow m_{i1} + \epsilon$ for $1 < i \leq n$. Since $B^{-1} = \text{diag}(m_{12}, \dots, m_{1n})$,

$$597 \quad \tilde{u}_1 - u_1 = -\frac{\epsilon u_1 e_1^\top L^\#(e_1 - e_i)}{1 + \epsilon e_1^\top L^\#(e_1 - e_i)} = \frac{\epsilon u_1 e_1^\top L^\#(e_i - e_1)}{1 - \epsilon e_1^\top L^\#(e_i - e_1)} = \frac{-\epsilon u_1^2 \bar{\mathbb{1}}^\top B^{-1} \bar{e}_{i-1}}{1 + \epsilon u_1 \bar{\mathbb{1}}^\top B^{-1} \bar{e}_{i-1}}$$

$$598 \quad = -\frac{\epsilon u_1^2 / m_{1i}}{1 + \epsilon u_1 / m_{1i}} < 0.$$

599 Since $u = \frac{1}{n} \mathbb{1}$, this gives $\tilde{u}_1 - u_1 = -\frac{1}{n} \frac{\epsilon / (nm_{1i})}{1 + \epsilon / (nm_{1i})}$. Since m_{1n} is the smallest among
 600 $\{m_{1k} : 2 \leq k \leq n\}$, the minimum of $\tilde{u}_1 - u_1$ is achieved at $k = n$, i.e.,

$$601 \quad \min_{2 \leq k \leq n} (\tilde{u}_1 - u_1) = -\frac{1}{n} \frac{\epsilon / (nm_{1n})}{1 + \epsilon / (nm_{1n})}.$$

602 This result indicates that the optimal strategy to reduce the infection risk is to increase
 603 m_{n1} when $m_{1k} = m_{k1}$ for all k .

604 Additionally, we claim that, in this special case where only changing weights
 605 between leaves is permitted, then the best strategy is to increase m_{n2} , as we now
 606 show. Perturbing $m_{ij} \rightarrow m_{ij} + \epsilon$ for $2 \leq i \neq j \leq n$, we find that

$$607 \quad (6.5) \quad \tilde{u}_1 - u_1 = -\frac{\epsilon u_j e_1^\top L^\#(e_j - e_i)}{1 + \epsilon e_j^\top L^\#(e_j - e_i)}$$

$$= \frac{\epsilon u_1 u_j \bar{\mathbb{1}}^\top B^{-1} (\bar{e}_{j-1} - \bar{e}_{i-1})}{1 + \epsilon \bar{e}_{j-1}^\top [B^{-1} (\bar{e}_{j-1} - \bar{e}_{i-1}) - \bar{u} \bar{\mathbb{1}}^\top B^{-1} (\bar{e}_{j-1} - \bar{e}_{i-1})]}$$

$$= \frac{\epsilon \frac{1}{n^2} \left(\frac{1}{m_{1j}} - \frac{1}{m_{1i}} \right)}{1 + \epsilon \left(\frac{1}{m_{1j}} - \frac{1}{n} \left(\frac{1}{m_{1j}} - \frac{1}{m_{1i}} \right) \right)} = \frac{\epsilon \frac{1}{n^2} (m_{1i} - m_{1j})}{m_{1i} m_{1j} + \epsilon \frac{1}{n} ((n-1)m_{1i} + m_{1j})}.$$

608 Note that $\tilde{u}_1 - u_1 < 0$ only if $i > j$ and hence this is the only interesting case.

609 It is straightforward to show that $\frac{\epsilon \frac{1}{n^2} (m_{1i} - m_{1j})}{m_{1i} m_{1j} + \epsilon \frac{1}{n} ((n-1)m_{1i} + m_{1j})}$ is increasing
 610 in m_{1i} and decreasing in m_{1j} . Thus the minimum is obtained at $i = n$ and $j = 2$.

611 Hence, $\min_{1 \leq j < i \leq n} (\tilde{u}_1 - u_1) = \frac{\epsilon \frac{1}{n^2} (m_{1n} - m_{12})}{m_{1n} m_{12} + \epsilon \frac{1}{n} ((n-1)m_{1n} + m_{12})}$ which implies that
 612 the most effective strategy to reduce the risk of infection is to increase m_{n2} .

613

614 *Case 2: the hot spot is located on a leaf (vertex $\ell \neq 1$):*

615 We claim that the best strategy is to increase m_{n1} when $\frac{m_{1\ell}}{m_{1n}} > n - 1$ and $n \neq \ell$, and

616 to increase $m_{1\ell}$ when $\frac{m_{1\ell}}{m_{1n}} < n - 1$, as we now show. Perturbing $m_{1\ell} \rightarrow m_{1\ell} + \epsilon$ yields

$$617 \quad (6.6) \quad \begin{aligned} \tilde{u}_\ell - u_\ell &= -\frac{\epsilon u_\ell e_\ell^\top L^\#(e_\ell - e_1)}{1 + \epsilon e_\ell^\top L^\#(e_\ell - e_1)} = -\frac{\epsilon u_\ell e_{\ell-1}^\top (B^{-1}\bar{e}_{\ell-1} - \bar{u}\bar{\mathbb{1}}^\top B^{-1}\bar{e}_{\ell-1})}{1 + \epsilon \bar{e}_{\ell-1}^\top (B^{-1}\bar{e}_{\ell-1} - \bar{u}\bar{\mathbb{1}}^\top B^{-1}\bar{e}_{\ell-1})} \\ &= -\frac{\epsilon u_\ell(1 - u_\ell)/m_{1\ell}}{1 + \epsilon(1 - u_\ell)/m_{1\ell}} = -\frac{1}{n} \frac{\epsilon \frac{n-1}{n} \frac{1}{m_{1\ell}}}{1 + \epsilon \frac{n-1}{n} \frac{1}{m_{1\ell}}} < 0. \end{aligned}$$

618 Perturbing $m_{i1} \rightarrow m_{i1} + \epsilon$ leads to

$$619 \quad \tilde{u}_\ell - u_\ell = -\frac{\epsilon u_1 e_\ell^\top L^\#(e_1 - e_i)}{1 + \epsilon e_1^\top L^\#(e_1 - e_i)} = \frac{\epsilon u_1 e_\ell^\top L^\#(e_i - e_1)}{1 - \epsilon e_1^\top L^\#(e_i - e_1)}.$$

620 Hence, if $i \neq \ell$, $\tilde{u}_\ell - u_\ell = \frac{\epsilon u_1 \bar{e}_{\ell-1}^\top (B^{-1}\bar{e}_{i-1} - \bar{u}\bar{\mathbb{1}}^\top B^{-1}\bar{e}_{i-1})}{1 + \epsilon u_1 \bar{\mathbb{1}}^\top B^{-1}\bar{e}_{i-1}} = -\frac{1}{n} \frac{\frac{\epsilon}{n} \frac{1}{m_{1i}}}{1 + \frac{\epsilon}{n} \frac{1}{m_{1i}}} < 0$,

621 and if $i = \ell$, $\tilde{u}_\ell - u_\ell = \frac{\epsilon u_1 \bar{e}_{\ell-1}^\top (B^{-1}\bar{e}_{\ell-1} - \bar{u}\bar{\mathbb{1}}^\top B^{-1}\bar{e}_{\ell-1})}{1 + \epsilon u_1 \bar{\mathbb{1}}^\top B^{-1}\bar{e}_{\ell-1}} = \frac{n-1}{n} \frac{\frac{\epsilon}{n} \frac{1}{m_{1\ell}}}{1 + \frac{\epsilon}{n} \frac{1}{m_{1\ell}}} > 0$. If

622 $i \neq \ell$, then the minimum of $\tilde{u}_\ell - u_\ell$ is achieved at $i = n$. To compare the two different
623 strategies (i.e., $m_{1\ell}$ and m_{n1}), we have the following conclusion: If $m_{1\ell}/m_{1n} < n - 1$,
624 the most effective strategy is to increase $m_{1\ell}$; If $m_{1\ell}/m_{1n} > n - 1$, the most effective
625 strategy is to increase m_{n1} provided that $n \neq \ell$.

626 **6.2. River with a hot spot.** As in section 6.1, we introduce a simplifying
627 hypothesis in order to make the analysis more tractable. We assume that $\alpha = 1$ (i.e.,
628 $a = b$), and observe that when this is the case, $u = \frac{1}{n}\mathbb{1}$.

629 We now have the following result.

630 LEMMA 6.1. *Suppose that $1 \leq i < j \leq n$. If $\alpha = 1$, then*

$$631 \quad e_k^\top L^\#(e_j - e_i) = \begin{cases} -\frac{1}{2n}(j-i)(2n-i-j+1), & 1 \leq k \leq i, \\ (k-j) + \frac{1}{2n}(j-i)(i+j-1), & i < k \leq j, \\ \frac{1}{2n}(j-i)(i+j-1), & j < k \leq n. \end{cases}$$

632 *Remark 6.1.* By Lemma 6.1 and equation (5.7), it is clear that $\tilde{u}_k - u_k$ is a
633 continuous, piecewise linear function and decreasing in k for $1 \leq k \leq n$. For $1 \leq k \leq i$,
634 $\tilde{u}_k - u_k$ is positive and constant in k , while for $j \leq k \leq n$, $\tilde{u}_k - u_k$ is negative and
635 constant in k .

636 Assume that we have distinct indices i, j with $1 \leq i, j \leq n$. By (6.4), to minimize
637 the infection risk, it suffices to minimize $\tilde{u}_\ell - u_\ell$, where ℓ is the hot spot. Perturb
638 $m_{ij} \rightarrow m_{ij} + \epsilon$ with $\epsilon > 0$. We have

$$639 \quad \tilde{u}_\ell - u_\ell = -\frac{\epsilon u_j e_\ell^\top L^\#(e_j - e_i)}{1 + \epsilon(L_{jj}^\# - L_{ji}^\#)} := -u_j g(i, j).$$

640 When $\alpha = 1$, $u_i = \frac{1}{n}$ for all $1 \leq i \leq n$ and $\min_{i,j,i \neq j}(\tilde{u}_\ell - u_\ell) = -\frac{1}{n} \max_{i,j,i \neq j} g(i, j)$.

641 Hence, minimizing $\tilde{R}_0 - R_0$ is equivalent to maximizing $g(i, j)$ over distinct i and j
642 with $1 \leq i, j \leq n$. It turns out that if $\ell \geq \frac{n+1}{2}$, then $\max_{i,j=1,\dots,n,i \neq j} g(i, j) =$

643 $\frac{\epsilon \ell(\ell-1)}{2n + \epsilon \ell(\ell-1)}$, with the maximum being attained when $i = 1, j = \ell$, while if $\ell \leq$

644 $\frac{n+1}{2}$, then $\max_{i,j=1,\dots,n,i\neq j} g(i,j) = \frac{\epsilon(n+1-\ell)(n-\ell)}{2n+\epsilon(n+1-\ell)(n-\ell)}$, with the maximum
 645 being attained when $i=n, j=\ell$. (See Supplementary Material (C) for the details.)
 646 Consequently, the most effective strategy to reduce the risk of infection is to increase
 647 $m_{1\ell}$ if the distance between vertices 1 and ℓ is at least as large as the distance between
 648 vertices n and ℓ , and to increase $m_{n\ell}$ otherwise.

649 On the other hand, if $1 \leq i < j \leq n$ are fixed, by Lemma 6.1, $\min_{\ell}(\tilde{u}_{\ell} - u_{\ell})$ can
 650 be achieved at any $j \leq \ell \leq n$. Thus, for fixed $i < j$, an increase in m_{ij} will have an
 651 equal and largest effect when the hot spot ℓ is such that $\ell \geq j$.

652 **7. Concluding remarks.** Our study, which focuses on disease dynamics, is
 653 motivated by modeling directly transmitted diseases [1] and waterborne diseases [17,
 654 44] on patches, under the hypothesis that dispersal between patches is faster than
 655 the disease/population dynamics. Our results also shed new insights on many spatial
 656 ecological studies, for example, the evolution of dispersal in patchy landscapes as
 657 studied in [2, 27] in a discrete time model.

658 Our methods give qualitative and quantitative information about the behavior of
 659 the basic reproduction number \mathcal{R}_0 as the topology of the network changes, and have
 660 applications to control strategies for mitigating disease spread among the patches.
 661 Our analysis can be thought of as the introduction of connections on the network, or
 662 changing the weight of existing connections. In the case that the change in a weight
 663 is positive, we have considered optimal strategies for a star and a river network. Our
 664 formula (4.2) is valid for all positive perturbations of a network connection, but a
 665 negative perturbation must be small for this to remain valid. Optimal strategies
 666 can also be formulated for a small negative change, as long as the network remains
 667 strongly connected. The effect of breaking this strong connectivity, and thus breaking
 668 the network topology, remains to be considered.

669 In patch models, the monotonicity of \mathcal{R}_0 with respect to travel frequency or the
 670 diffusion coefficient on a static network has been studied in several papers, for ex-
 671 ample [1, 18]; by contrast our results focus on the network topology. The network
 672 threshold parameter \mathcal{R}_0 governs the invasibility of the disease, but not the final size or
 673 endemicity of an invading disease. To consider this, it is necessary to use the original
 674 dynamical model.

675

676 Acknowledgments.

677 The authors thank the American Institute of Mathematics (AIM) for its hosting
 678 and generous support of an AIM SQuaRE program focusing on epidemic dynamics of
 679 cholera in non-homogeneous environments, at which this research was initiated and
 680 developed. The authors also thank the anonymous reviewers for helpful suggestions.

681

REFERENCES

- 682 [1] L. J. S. ALLEN, B. M. BOLKER, Y. LOU, AND A. L. NEVAI, *Asymptotic profiles of the steady*
 683 *states for an SIS epidemic patch model*, SIAM J. Appl. Math., 67 (2007), pp. 1283–1309.
 684 [2] L. ALTENBERG, *Resolvent positive linear operators exhibit the reduction phenomenon*, Proc.
 685 Natl. Acad. Sci. USA, 109 (2012), pp. 3705–3710.
 686 [3] M. Y. ANWAR, J. L. WARREN, AND V. E. PITZER, *Diarrhea patterns and climate: A spatiotem-*
 687 *poral Bayesian hierarchical analysis of diarrheal disease in Afghanistan*, American Journal
 688 of Tropical Medicine and Hygiene, 101 (2019), pp. 525–533.
 689 [4] M. BAQIR, Z. A. SOBANI, A. BHAMANI, N. S. BHAM, S. ABID, J. FAROOK, AND M. A. BEG,
 690 *Infectious diseases in the aftermath of monsoon flooding in Pakistan*, Asian Pacific Journal
 691 of Tropical Biomedicine, 2 (2012), pp. 76–79.

- 692 [5] A. BERMAN AND R. PLEMMONS, *Nonnegative Matrices in the Mathematical Sciences*, Society
693 for Industrial and Applied Mathematics, Philadelphia, PA, 1994.
- 694 [6] E. BERTUZZO, L. MARI, L. RIGHETTO, M. GATTO, R. CASAGRANDI, I. RODRIGUEZ-ITURBE,
695 AND A. RINALDO, *Hydroclimatology of dual-peak annual cholera incidence: insights from
696 a spatially explicit model*, Geophysical Research Letters, 39 (2012).
- 697 [7] S. L. CAMPBELL AND C. D. MEYER, *Generalized Inverses of Linear Transformations*, Society
698 for Industrial and Applied Mathematics, Philadelphia, PA, 2009.
- 699 [8] R. S. CANTRELL, C. COSNER, M. A. LEWIS, AND Y. LOU, *Evolution of dispersal in spatial
700 population models with multiple timescales*, J. Math. Biol., Published online, [https://doi.
701 org/10.1007/s00285-018-1302-2](https://doi.org/10.1007/s00285-018-1302-2).
- 702 [9] E. J. CARLTON, J. N. EISENBERG, J. GOLDSTICK, W. CEVALLOS, J. TROSTLE, AND K. LEVY,
703 *Heavy rainfall events and diarrhea incidence: the role of social and environmental factors*,
704 American Journal of Epidemiology, 179 (2013), pp. 344–352.
- 705 [10] M. CARREL, P. VOSS, P. K. STREATFIELD, M. YUNUS, AND M. EMCH, *Protection from an-
706 nual flooding is correlated with increased cholera prevalence in Bangladesh: a zero-inflated
707 regression analysis*, Environmental Health, 9 (2010), p. 13.
- 708 [11] S. CHAIKEN, *A combinatorial proof of the all minors matrix tree theorem*, SIAM J. Algebraic
709 Discrete Methods, 3 (1982), pp. 319–329.
- 710 [12] S. CHEN, J. SHI, Z. SHUAI, AND Y. WU, *Spectral monotonicity of perturbed quasi-positive
711 matrices with applications in population dynamics*, arXiv preprint arXiv:1911.02232.
- 712 [13] F. C. CURRIERO, J. A. PATZ, J. B. ROSE, AND S. LELE, *The association between extreme
713 precipitation and waterborne disease outbreaks in the United States, 1948–1994*, American
714 Journal of Public Health, 91 (2001), pp. 1194–1199.
- 715 [14] E. DEUTSCH AND M. NEUMANN, *On the first and second order derivatives of the perron vector*,
716 Linear Algebra Appl., 71 (1985), pp. 57–76.
- 717 [15] M. DHIMAL, B. AHRENS, AND U. KUCH, *Climate change and spatiotemporal distributions of
718 vector-borne diseases in Nepal—a systematic synthesis of literature*, PLOS One, 10 (2015),
719 p. e0129869.
- 720 [16] M. C. EISENBERG, G. KUJBIDA, A. R. TUIITE, D. N. FISMAN, AND J. H. TIEN, *Examining
721 rainfall and cholera dynamics in Haiti using statistical and dynamic modeling approaches*,
722 Epidemics, 5 (2013), pp. 197–207.
- 723 [17] M. C. EISENBERG, Z. SHUAI, J. H. TIEN, AND P. VAN DEN DRIESSCHE, *A cholera model in a
724 patchy environment*, Math. Biosci., 246 (2013), pp. 105–112.
- 725 [18] D.-Z. GAO, *Travel frequency and infectious diseases*, SIAM J. Appl. Math., 79 (2019), pp. 1581–
726 1606.
- 727 [19] D.-Z. GAO AND C.-P. DONG, *Fast diffusion inhibits disease outbreaks*, arXiv preprint
728 arXiv:1907.12229.
- 729 [20] M. GATTO, L. MARI, E. BERTUZZO, R. CASAGRANDI, L. RIGHETTO, I. RODRIGUEZ-ITURBE, AND
730 A. RINALDO, *Generalized reproduction numbers and the prediction of patterns in water-
731 borne disease*, Proceedings of the National Academy of Sciences, 109 (2012), pp. 19703–
732 19708.
- 733 [21] A. GAUDIELLO, *Mathematical Investigation of the Spatial Spread of an Infectious Disease in a
734 Heterogeneous Environment*, PhD thesis, University of Central Florida, 2019.
- 735 [22] S. GOURLEY, R. LIU, AND J. WU, *Spatiotemporal patterns of disease spread: Interaction of
736 physiological structure, spatial movements, disease progression and human intervention*,
737 in Structured Population Models in Biology and Epidemiology, Springer, 2008, pp. 165–
738 208.
- 739 [23] M. HASHIZUME, B. ARMSTRONG, S. HAJAT, Y. WAGATSUMA, A. S. FARUQUE, T. HAYASHI, AND
740 D. A. SACK, *The effect of rainfall on the incidence of cholera in Bangladesh*, Epidemiology,
741 19 (2008), pp. 103–110.
- 742 [24] R. A. HORN AND C. R. JOHNSON, *Matrix Analysis*, Cambridge University Press, Cambridge,
743 2013.
- 744 [25] S. KARLIN, *Classifications of selection-migration structures and conditions for a protected poly-
745 morphism*, in Evolutionary Biology, vol. 14, Plenum Press, New York, 1982, pp. 61–204.
- 746 [26] R. B. KAUL, M. V. EVANS, C. C. MURDOCK, AND J. M. DRAKE, *Spatio-temporal spillover risk
747 of yellow fever in Brazil*, Parasites & Vectors, 11 (2018), p. 488.
- 748 [27] S. KIRKLAND, C.-K. LI, AND S. J. SCHREIBER, *On the evolution of dispersal in patchy land-
749 scapes*, SIAM J. Appl. Math., 66 (2006), pp. 1366–1382.
- 750 [28] S. J. KIRKLAND AND M. NEUMANN, *Group Inverses of M -Matrices and their Applications*,
751 CRC Press, Boca Raton, FL, 2013.
- 752 [29] K. LEVY, S. M. SMITH, AND E. J. CARLTON, *Climate change impacts on waterborne diseases:
753 moving toward designing interventions*, Current Environmental Health Reports, 5 (2018),

- 754 pp. 272–282.
- 755 [30] K. LEVY, A. P. WOSTER, R. S. GOLDSTEIN, AND E. J. CARLTON, *Untangling the impacts*
756 *of climate change on waterborne diseases: a systematic review of relationships between*
757 *diarrheal diseases and temperature, rainfall, flooding, and drought*, *Environmental Science*
758 *& Technology*, 50 (2016), pp. 4905–4922.
- 759 [31] A. LÓPEZ-QUÍLEZ, *Spatio-temporal analysis of infectious diseases*, *International Journal of En-*
760 *vironmental Research and Public Health*, 16 (2019), p. 669.
- 761 [32] M. Á. LUQUE FERNÁNDEZ, A. BAUERNFEIND, J. D. JIMÉNEZ, C. L. GIL, N. E. OMEIRI, AND
762 D. H. GUIBERT, *Influence of temperature and rainfall on the evolution of cholera epidemics*
763 *in Lusaka, Zambia, 2003–2006: analysis of a time series*, *Transactions of the Royal Society*
764 *of Tropical Medicine and Hygiene*, 103 (2009), pp. 137–143.
- 765 [33] L. MARI, R. CASAGRANDE, E. BERTUZZO, A. RINALDO, AND M. GATTO, *Conditions for transient*
766 *epidemics of waterborne disease in spatially explicit systems*, *Royal Society Open Science*,
767 6 (2019), p. 181517.
- 768 [34] C. D. MEYER, *The condition of a finite markov chain and perturbation bounds for the limiting*
769 *probabilities*, *SIAM J. Algebraic Discrete Methods*, 1 (1980), pp. 273–283.
- 770 [35] C. D. MEYER, *Matrix Analysis and Applied Linear Algebra*, SIAM, 2000.
- 771 [36] J. W. MOON, *Counting Labelled Trees*, Canadian Mathematical Congress, Montreal, Canada,
772 1970.
- 773 [37] M. H. MYER AND J. M. JOHNSTON, *Spatiotemporal Bayesian modeling of West Nile virus:*
774 *Identifying risk of infection in mosquitoes with local-scale predictors*, *Science of the Total*
775 *Environment*, 650 (2019), pp. 2818–2829.
- 776 [38] J. OKPASUO, F. OKAFOR, AND I. AGUZIE, *Effects of household drinking water choices, knowl-*
777 *edge, practices and spatio-temporal trend on the prevalence of waterborne diseases in*
778 *Enugu Urban, Nigeria*, *International Journal of Infectious Diseases*, 73 (2018), pp. 225–226.
- 779 [39] M. G. ROSA-FREITAS, N. A. HONÓRIO, C. T. CODEÇO, G. L. WERNECK, AND N. DEGALLIER,
780 *Spatial studies on vector-transmitted diseases and vectors*, *Journal of Tropical Medicine*,
781 2012 (2012).
- 782 [40] G. ROSSI, S. KARKI, R. L. SMITH, W. M. BROWN, AND M. O. RUIZ, *The spread of mosquito-*
783 *borne viruses in modern times: A spatio-temporal analysis of dengue and chikungunya*,
784 *Spatial and Spatio-Temporal Epidemiology*, 26 (2018), pp. 113–125.
- 785 [41] M. S. SARFRAZ, N. K. TRIPATHI, T. TIPDECHO, T. THONGBU, P. KERDTHONG, AND M. SOURIS,
786 *Analyzing the spatio-temporal relationship between dengue vector larval density and land-*
787 *use using factor analysis and spatial ring mapping*, *BMC Public Health*, 12 (2012), p. 853.
- 788 [42] W. SUN, L. XUE, AND X. XIE, *Spatio-temporal distribution of dengue and climate charac-*
789 *teristics for two clusters in Sri Lanka from 2012 to 2016*, *Scientific Reports*, 7 (2017),
790 p. 12884.
- 791 [43] A. J. TATEM, D. J. ROGERS, AND S. I. HAY, *Global transport networks and infectious disease*
792 *spread*, *Advances in Parasitology*, 62 (2006), pp. 293–343.
- 793 [44] J. H. TIEN, Z. SHUAI, M. C. EISENBERG, AND P. VAN DEN DRIESSCHE, *Disease invasion on*
794 *community networks with environmental pathogen movement*, *J. Math. Biol.*, 70 (2015),
795 pp. 1065–1092.
- 796 [45] A. VENKAT, T. M. A. FALCONI, M. CRUZ, M. A. HARTWICK, S. ANANDAN, N. KUMAR,
797 H. WARD, B. VEERARAGHAVAN, AND E. N. NAUMOVA, *Spatiotemporal patterns of cholera*
798 *hospitalization in Vellore, India*, *International Journal of Environmental Research and*
799 *Public Health*, 16 (2019), p. 4257.
- 800 [46] L. S. WALDRON, B. DIMESKI, P. J. BEGGS, B. C. FERRARI, AND M. L. POWER, *Molecular*
801 *epidemiology, spatiotemporal analysis, and ecology of sporadic human cryptosporidiosis in*
802 *Australia*, *Appl. Environ. Microbiol.*, 77 (2011), pp. 7757–7765.
- 803 [47] L. A. WALLER, B. J. GOODWIN, M. L. WILSON, R. S. OSTFELD, S. L. MARSHALL, AND E. B.
804 HAYES, *Spatio-temporal patterns in county-level incidence and reporting of lyme disease*
805 *in the northeastern United States, 1990–2000*, *Environmental and Ecological Statistics*, 14
806 (2007), p. 83.

807 **Supplementary Material.** (A) A version of the multi-patch cholera model in [17,
808 44], simplified by ignoring host movement, takes the following form:

$$\begin{aligned} \frac{dS_i}{dt} &= A_i - g_i(S_i, W_i) - d_i S_i, \\ \frac{dI_i}{dt} &= g_i(S_i, W_i) - (d_i + \alpha_i + \gamma_i) I_i, \\ \frac{dR_i}{dt} &= \gamma_i I_i - d_i R_i, \\ \frac{dW_i}{dt} &= r_i I_i - \delta_i W_i + \sum_{j=1}^n (m_{ij} W_j - m_{ji} W_i), \end{aligned}$$

with variables and parameters summarized in the following list:

- S_i, I_i, R_i : susceptible, infectious and recovered host population in patch i
- W_i : the concentration of cholera bacteria in the water source in patch i
- $A_i > 0$: constant recruitment into patch i
- $d_i > 0$: natural death rate in patch i
- $\alpha_i \geq 0$: cholera induced death rate in patch i
- $\gamma_i > 0$: recovery rate of infectious individuals in patch i
- $r_i \geq 0$: pathogen shedding rate in patch i
- $\delta_i > 0$: removal rate of pathogen in patch i
- $m_{ij} \geq 0$: travel rate of pathogen from patch j to patch i
- $g_i(S_i, W_i) \geq 0$: incidence function for cholera transmission in patch i

810 Linearization at the disease-free equilibrium $(\frac{A_1}{d_1}, 0, 0, 0, \dots, \frac{A_n}{d_n}, 0, 0, 0)$ and reducing
811 to the disease compartments (i.e., I_i and W_i) yield the Jacobian matrix $J = F - V$ with
812 $F = \begin{pmatrix} 0 & D_q \\ 0 & 0 \end{pmatrix}$ and $V = \begin{pmatrix} G_I & 0 \\ -D_r & G_W \end{pmatrix}$. Here $D_q = \text{diag}\{q_i\} := \text{diag}\{\frac{\partial g_i}{\partial W_i}(\frac{A_i}{d_i}, 0)\}$,
813 $G_W = \text{diag}\{\delta_i\} + L$ with L being the Laplacian matrix as defined in (2.1), $D_r =$
814 $\text{diag}\{r_i\}$ and $G_I = \text{diag}\{\mu_i\} := \text{diag}\{d_i + \alpha_i + \gamma_i\}$. Thus the basic reproduction
815 number \mathcal{R}_0 is defined as the spectral radius of the next generation matrix FV^{-1} ; that
816 is, $\mathcal{R}_0 = \rho(FV^{-1}) = \rho(D_q G_W^{-1} D_r G_I^{-1})$.

817 For directly transmitted disease models such as the SIS model in [1], the basic
818 reproduction number $\mathcal{R}_0 = \rho(\text{diag}\{\beta_i\}(\text{diag}\{\eta_i\} + d_I L)^{-1})$, where β_i is the disease
819 transmission coefficient for the standard incidence, η_i is the rate of infectious indi-
820 viduals becoming susceptible again, and d_I represents the scale of movement rate of
821 infectious individuals.

822 (B) Suppose that \hat{L} is given by (5.5). We claim that it suffices to consider the
823 case that $a \geq b$. To see the claim, first note that $\hat{L} = P\bar{L}P^\top$, where

$$\bar{L} = \begin{pmatrix} b & -a & 0 & \cdots & 0 & 0 \\ -b & a+b & -a & \cdots & 0 & 0 \\ 0 & -b & a+b & \cdots & 0 & 0 \\ \vdots & \vdots & & & & \\ 0 & 0 & 0 & \cdots & a+b & -a \\ 0 & 0 & 0 & \cdots & -b & a \end{pmatrix}$$

825 and P is the $n \times n$ ‘‘back diagonal’’ permutation matrix such that $p_{j, n+1-j} = 1, j =$
826 $1, \dots, n$. If it happens that $a < b$, we then work with \bar{L} instead of \hat{L} .

827 (C) Here we derive the expression for $\max_{i,j=1,\dots,n,i \neq j} g(i,j)$ given at the end of
 828 section 6.2. We begin by supposing that $1 \leq i < j \leq n$. If $1 \leq \ell \leq i$, then by Lemma
 829 6.1, $g(i,j) = \frac{\epsilon \left[-\frac{1}{2n}(j-i)(2n-i-j+1) \right]}{1 + \epsilon \frac{1}{2n}(j-i)(i+j-1)}$. Hence, for $1 \leq \ell \leq i$, the maximum value
 830 of $g(i,j)$ is achieved when $i = n-1$ and $j = n$, with $g(n-1,n) = -\frac{\epsilon}{n + \epsilon(n-1)}$.

831 If $j \leq \ell \leq n$, then by Lemma 6.1, $g(i,j) = \frac{\epsilon \left[\frac{1}{2n}(j-i)(i+j-1) \right]}{1 + \epsilon \frac{1}{2n}(j-i)(i+j-1)}$. Thus when
 832 $j \leq \ell \leq n$, the maximum value of $g(i,j)$ is achieved when $j = \ell$ and $i = 1$, with
 833 $g(1,\ell) = \frac{\epsilon \ell(\ell-1)}{2n + \epsilon \ell(\ell-1)}$.

834 For the intermediate case where $i < \ell \leq j$, using Lemma 6.1, we have

$$835 \quad g(i,j) = \frac{\epsilon \left[(\ell-j) + \frac{1}{2n}(j-i)(i+j-1) \right]}{1 + \epsilon \frac{1}{2n}(j-i)(i+j-1)} \leq \frac{\epsilon \left[\frac{1}{2n}(j-i)(i+j-1) \right]}{1 + \epsilon \frac{1}{2n}(j-i)(i+j-1)}.$$

836 From the considerations above, it follows that for $1 \leq i < j \leq n$, the maximum value
 837 of $g(i,j)$ is $\frac{\epsilon \ell(\ell-1)}{2n + \epsilon \ell(\ell-1)}$, which is achieved when $j = \ell$ and $i = 1$.

Next, consider the case that $1 \leq j < i \leq n$. A parallel argument (which pro-
 ceeds by considering the indices $n+1-j, n+1-i$ and $n+1-\ell$) shows that
 $\max_{1 \leq j < i \leq n} g(i,j) = \frac{\epsilon(n+1-\ell)(n-\ell)}{2n + \epsilon(n+1-\ell)(n-\ell)}$. We deduce that

$$\max_{i,j=1,\dots,n,i \neq j} g(i,j) = \max \left\{ \frac{\epsilon \ell(\ell-1)}{2n + \epsilon \ell(\ell-1)}, \frac{\epsilon(n+1-\ell)(n-\ell)}{2n + \epsilon(n+1-\ell)(n-\ell)} \right\}.$$

838 More specifically, if $\ell \geq \frac{n+1}{2}$, then $\max_{i,j=1,\dots,n,i \neq j} g(i,j) = \frac{\epsilon \ell(\ell-1)}{2n + \epsilon \ell(\ell-1)}$, and
 839 the maximum is attained for $i = 1, j = \ell$; on the other hand, if $\ell \leq \frac{n+1}{2}$, then
 840 $\max_{i,j=1,\dots,n,i \neq j} g(i,j) = \frac{\epsilon(n+1-\ell)(n-\ell)}{2n + \epsilon(n+1-\ell)(n-\ell)}$, and the maximum is attained for
 841 $i = n, j = \ell$.